

Bone & Soft Tissue

analysis, only age ($p=.008$), body mass index ($p<.0001$) and presence of healed infarct ($p=.06$) were associated with cardiomegaly score, extent of coronary disease showing no correlation ($p=0.9$).

Conclusions: There is no significant correlation between extent of coronary atherosclerosis and cardiac hypertrophy independent of age and body mass index in sudden coronary deaths. These data do not support a causative association between chronic ischemia and cardiomegaly.

16 Nonspecific Cardiomyopathy: A Common Cause of Death with a Need for Standardization of Terminology.

J Shields, L Li, DR Fowler, Y Zhang, AP Burke. University of Maryland, Baltimore; Maryland Office of the Chief Medical Examiner, Baltimore; University of Maryland School of Medicine, Baltimore.

Background: The terminology and classification of sudden cardiac deaths in patients with cardiomegaly as the primary cause of death have not been clarified.

Design: A retrospective review of autopsy records from a single calendar year at a state-wide medical examiner's office was performed. Cases of sudden cardiac deaths were retained for study. Causes of death and cardiac findings were tabulated, and cases with potential noncardiac causes, such as drug and alcohol related deaths, were excluded. Cases with coronary atherosclerotic disease (≥ 1 vessel with $\geq 75\%$ luminal area narrowing) were excluded. Cardiomegaly was determined based on body height and weight; mild cardiomegaly was defined as < 50 grams above the 95% upper limit; moderate: 50-99 grams; marked: 100-200 grams; and massive: > 200 grams above the limit, respectively. The incidence, demographics and terminology applied for these deaths was analyzed.

Results: Among 484 sudden cardiac deaths, 241 deaths (50%) had severe atherosclerosis, 41 arrhythmia/sudden adult death syndrome (8%), 15 valvular disease (3%), 19 inflammatory or specific cardiomyopathy (4%) and 5 miscellaneous causes (1%). 161 deaths were due to nonspecific cardiomyopathy (NSC) (33%). Hypertrophic cardiomyopathy was excluded based on the lack of septal asymmetry and myofiber disarray. Of NSC cases, the mean age was 46 ± 12 years; there were 104 males and 57 females; 45% were African American. A history of hypertension was present in 66 cases (47%). The mean body mass index (BMI) was 33.5 ± 10.6 . The mean heart weight was 572 ± 150 g. Twelve percent of decedents had a remote history of alcohol abuse. Twenty-seven percent of the nonspecific cardiomyopathy deaths were witnessed and 1.2% were exertion related deaths. The autopsy reports listed a variety of terms, including left ventricular hypertrophy, arrhythmia associated with cardiomegaly, dilated cardiomegaly, hypertensive cardiovascular disease, and nonischemic cardiomyopathy.

Conclusions: Approximately one third of sudden cardiac deaths are secondary to nonspecific cardiomyopathy; however, a uniform nomenclature for the causes of death in these cases is lacking. The term nonspecific cardiomyopathy is recommended for use in such cases, with risk factors such as hypertension, obesity and alcoholism listed as contributing factors.

17 Integration of Autopsy Pathology and Genetics in Hunter Syndrome (MPSII).

LD Wood, MK Halushka, FB Askin, LC Racusen, RA Anders, B Baskin, PN Ray, T Van Kuppevelt, RG Wismans, BJ Crain, MR Natowicz, GS Bova. Johns Hopkins University School of Medicine, Baltimore, MD; The Hospital for Sick Children, Toronto, ON, Canada; Radboud University, Nijmegen Medical Centre, Netherlands; Cleveland Clinic, OH.

Background: Hunter syndrome (MPSII), a rare X-linked lysosomal storage disorder caused by germ-line mutations in the iduronate-2-sulfatase (*IDS*) gene, is a mucopolysaccharidosis characterized by abnormal accumulation of glycosaminoglycans (GAGs) in multiple organs. Although the clinical syndrome of MPSII is well described, systematic anatomic studies of its pathology are limited, and studies integrating gross and microscopic pathology with specific mutations have not been reported. Insights from these natural human mutations affecting GAG degradation could improve our understanding of the role of GAGs in health and disease.

Design: We performed comprehensive gross and microscopic analysis for 2 autopsy subjects with MPSII. Tissues were examined using H&E staining, colloidal iron staining, and a novel antibody specific for dermatan sulfate. We also performed DNA sequencing on all coding exons of the *IDS* gene in formalin-fixed paraffin-embedded lymphoid tissue from each patient.

Results: DNA sequencing of the *IDS* gene revealed different pathogenic mutations in each patient: one novel single-base deletion in exon 6 creating an in-frame stop codon (c.817delC, p.Arg273fsX) and one previously reported disease-causing missense mutation in exon 3 (c.253G>A, p.Ala85Thr). Gross examination of tissues at autopsy confirmed previously reported anatomic anomalies and identified novel findings, including coronary artery occlusion (not previously reported in MPSII) and choroid plexus fibrosis (not previously reported in any mucopolysaccharidosis). Microscopic examination revealed that abnormal vacuolated cells containing undegraded GAGs were present in multiple organs, including the heart, blood vessels, lungs, liver, kidney, and brain.

Conclusions: This study is the first to integrate systematic autopsy examination with specific mutations in MPSII, highlighting the power of genotype-phenotype correlation in the understanding of the pathogenesis of genetic disease. Moreover, we extend the current notion of genotype-phenotype analysis beyond clinical syndrome to include correlation of gross and microscopic pathology with specific mutations. Expansion of the methods used in this study to additional cases of MPSII could greatly enhance our understanding of the inherited disorders of GAG metabolism and GAG biology more generally.

18 Expression of Therapeutically Relevant Molecules in Ewing's Sarcoma Family Tumors.

A Ahmed, J Whiting, B Pawel. Children's Mercy Hospital, Kansas City, MO; Children's Hospital of Philadelphia, PA.

Background: Ewing sarcoma family tumor (EFT) is an aggressive malignant tumor of bone and soft tissue in children and adolescents. Modern treatment regimens are effective in localized disease. Metastasis occurs in 20-25% of cases and results in mortality in 80% of patients. New insight has led to identification of mTOR, AKT, VEGF and NF-kappa B as important kinases and transcription factors that regulate the proliferation of EFT tumor cells in vitro. BRAF is another kinase molecule that is over-expressed in numerous cancers and has not been previously studied in EFT.

Design: 72 cases with established diagnosis of EFT were selected. Survival data was available in 50 cases, classified as no evidence of disease (NED), alive with disease (AED) or died of disease (DOD). Formalin-fixed tumor sections were stained with antibodies against phosphorylated mTOR, AKT, BRAF, VEGF and NF-kappa B proteins. Stained sections were analyzed and graded for extent (percentage of stained cells) and strength of staining (negative [0], weak [1] or strong [2]). A composite score (from 0 to 200) was calculated by multiplying percentage of stained cells by strength of staining. The results were statistically correlated with patients' survival outcome.

Results: 1-4 cases were excluded because of insufficient viable tumor. The remaining cases (≥ 68) showed variable positive staining for the selected markers. Significant staining (score ≥ 100) was identified in 86% of cases stained for Akt, 55% of cases stained for NF-Kappa B, 37% of cases stained for m-TOR and only 12% of cases stained for VEGF. BRAF showed negative or weak staining (score < 100) in 97% of cases.

Decreased VEGF expression (score < 100) was significantly associated with NED, i.e. better prognosis ($p<0.05$). No significant association was demonstrated between the expression of the remaining proteins and the prognosis.

Conclusions: The majority of EFT cases express mTOR, AKT, VEGF and NF-kappa B proteins and do not express BRAF. EFT tumors may be amenable to treatment that targets the expressed proteins. High Akt expression suggests potential universal response to Akt-targeted therapy. BRAF kinase inhibitors are unlikely to be effective in the treatment of Ewing's sarcoma family tumors. VEGF expression is related to prognosis and larger studies may be needed to correlate VEGF over-expression to patients' prognosis and document the effectiveness of VEGF inhibitors in the treatment of these patients.

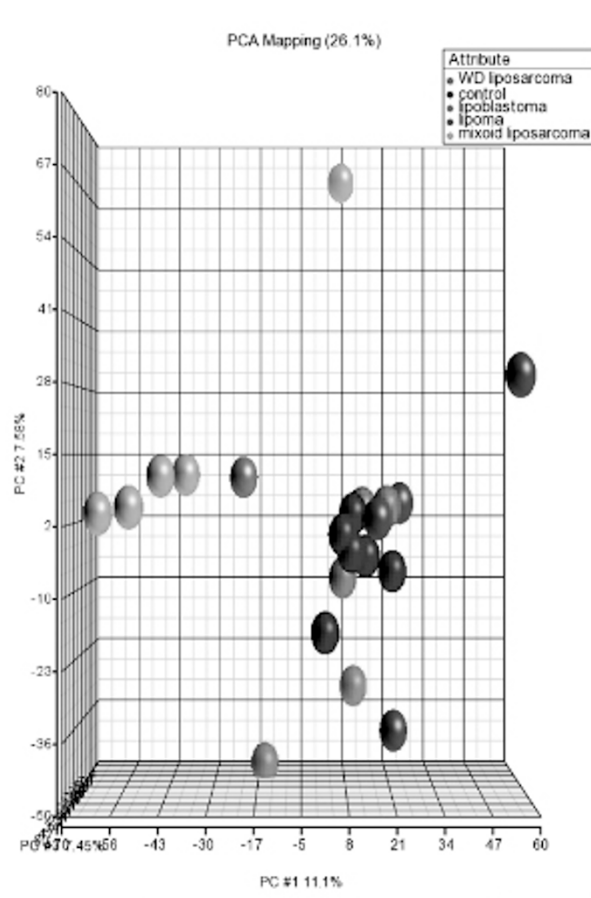
19 microRNA Profiling in Adipocytic Neoplasms.

WA Ahrens, NM Steuerwald, JC Patt, JS Kneisl, HL Bonkovsky. Carolinas Medical Center, Charlotte, NC.

Background: MicroRNAs (miRNAs) are a class of small noncoding RNAs. They have been shown to promote or suppress tumorigenesis in human cancers by altering cancer-related gene expression. Subtype-specific expression patterns are emerging in various types of sarcoma. In this study, miRNA expression profiling was performed in 18 adipocytic tumors.

Design: Snap-frozen tumor was collected from 7 well-differentiated liposarcomas (WDLs), 4 myxoid liposarcomas (MLS), 2 lipoblastomas (LB) and 5 lipomas (LP). Non-neoplastic adipose was collected in 6 cases as control. RNA was isolated using Qiagen miRNeasy. RNA was Poly A tailed and ligated to biotinylated signal molecules using the FlashTag Biotin RNA labeling Kit (Genisphere). An Enzyme Linked Oligosorbent Assay QC assay was performed to verify labeling prior to hybridization to GeneChip miRNA Arrays (Affymetrix, Santa Clara, CA). Hybridization, washing, staining and scanning was performed using Affymetrix GeneChip system instruments. Affymetrix GeneChip Operating Software version 1.4 was used to analyze microarray image data and to compute intensity values. Partek Genomic Suite (Partek Inc., St. Louis, MI, USA) was used to compute fold changes and perform statistical analyses.

Results: Tumor subtype principal component analysis is shown in figure 1.



The 4 MLS grouped closely together. >10 fold up-regulation vs control was observed for hsa-miRs 486-5p/451/29a and 150. >10 fold down regulation was observed for hsa-miRs 891a/181a/181c/493 and 1247. LB showed >10 fold up-regulation vs control for hsa-miRs 486-5p/451/1246 and 182. >10 fold down regulation was observed for hsa-miRs 433/493/409-5p/382/431/485-5p and 376c. 1 LB showed overlap of 14 individual miRs with the MLS cluster. WDLS and LP grouped with control cases. The p value for all fold changes was <0.05.

Conclusions: This data supports that notion that miRNA profiling can be used to subclassify adipocytic neoplasms with histologic overlap. Importantly, identification of specific miRNAs and their targets may reveal tumor markers with prognostic value as well as targets for treatment intervention in sarcoma.

20 Metastasizing Dedifferentiated Liposarcoma: Clinical and Morphologic Analysis.

TJ Al-Zaid, M Ghadimi, T Peng, C Colombo, KE Torres, D Lev, AJ Lazar. UT-MD Anderson Cancer Center, Houston, TX.

Background: Dedifferentiated liposarcoma consists of well differentiated (WD) liposarcoma with a dedifferentiated (DD) higher grade, non-lipogenic component. The majority of fatal cases are attributed to local aggressiveness. The incidence of distant metastasis reported in the literature is relatively low (1-18%) for retroperitoneal cases and predicts a rapidly fatal course.

Design: Patients with DD liposarcoma who developed distant metastasis (n=45) were identified in our liposarcoma database (total, n=491; de novo DD, n=197; secondary DD, n=62; WD only, n=232). H&E slides for 21 patients were available (remaining 24 are being acquired). A metastasis was defined as tumor involving a distinct, distant site. The dominant morphologic patterns of the DD component was classified as: myxofibrosarcoma(MFS)-like, malignant fibrous histiocytoma/pleomorphic undifferentiated sarcoma (MFH/UPS)-like, pleomorphic liposarcoma(PLS)-like, sarcoma with heterologous elements, pure pleomorphic, and epithelioid. The primary/recurrent DD component was graded per FNCLCC criteria. The highest grade observed from a primary/recurrent tumor from each patient was used for analysis.

Results: Patient age at primary liposarcoma diagnosis was 33 to 78 years including males (n=32) and females (n=13). Primary tumors were retroperitoneal (n=31; 69%), scrotal (n=4; 9%), pelvic/mesenteric (n=4; 9%), chest/abdominal wall (n=5; 11%), and mediastinal (n=1; 2%). 42 cases arose from de novo DD and 3 from secondary DD. The sites of metastasis include lung (n=34; 76%), liver (n=11; 24%), bone (n=3; 7%), brain (n=2; 4%), and other (n=3; 7%). Metastasis to more than one organ were present in 12 patients (27%). Of the 21 patients with histologic slides available, the DD component exhibited the following morphologic patterns (often multiple) in the primary tumor or recurrence: MFH/UPS-like (n=15; 72%), MFS-like (n=8; 38%), heterologous element osteosarcoma (n=3; 14%), pure pleomorphic (n=1; 5%). The DD component was FNCLCC high grade (n=2; 10%) or intermediate (n=19; 90%).

Conclusions: In our series, most metastases from DD liposarcoma originated from retroperitoneum (69%; the most prevalent primary site), scrotum (9%) and chest/

abdominal wall (11%). The most common metastatic sites were lung (76%) and liver (24%). The prevalent primary/recurrent DD component morphology was MFH/UPS-like (72%) followed by MFS-like (38%); most metastases arose from DD graded FNCLCC intermediate. The overall metastatic rate for DD liposarcoma was 17% (21% of de novo DD; 5% of secondary DD).

21 Consistent t(1;10) Abnormality in Both Myxoinflammatory Fibroblastic Sarcoma (MIFS) and Hemosiderotic Fibrolipomatous Tumor (HFLT).

CR Antonescu, L Zhang, GP Nielsen, AE Rosenberg, P Dal Cin, CD Fletcher. Memorial Sloan-Kettering Cancer Ctr, New York, NY; Massachusetts General Hospital, Boston; Brigham & Women's Hospital, Boston, MA.

Background: Despite their common predilection for superficial acral location and frequent local recurrences, MIFS and HFLT have distinct morphologic appearances. Only recently cytogenetic studies have identified the presence of an identical t(1;10) (p22;q24) in 5 cases of MIFS and 2 of HFLT, suggesting a pathogenetic link between these two entities.

Design: In order to investigate further the potential relationship between these lesions, as well as to determine the incidence of t(1;10) in a larger group of patients, we subjected 22 cases, representing 6 MIFS, 13 HFLT, and 3 cases with mixed morphology, to molecular and cytogenetic analysis. FISH analysis using custom BAC probes for *TGFBR3* on 1p22 and *MGEA5* on 10q24 was performed in all cases. Conventional karyotyping was also performed in one HFLT and two cases with mixed MIFS/HFLT histology.

Results: Overall 81% of cases (4/6 MIFS and 11/13 HFLT) showed gene rearrangements in both *TGFBR3* and *MGEA5*. A consistent unbalanced pattern was identified by FISH, with deletion of centromeric fragment of *TGFBR3* and telomeric portion of *MGEA5*. All three cases with features of MIFS and HFLT were positive. Two otherwise typical cases from each group, one each in the arm and leg, were negative for rearrangement in both genes by FISH. Cytogenetic analysis performed in three cases confirmed the presence of a t(1;10)(p22;q24), as well as loss of chromosome 3 material.

Conclusions: The high incidence of t(1;10) in both MIFS and HFLT reinforce the likely shared pathogenetic relationship of these two lesions. Furthermore, the co-existence of both components either synchronously within the same tumor or metachronously in primary/subsequent recurrence, suggest that they represent different morphologic variants of the same entity. FISH analysis for the presence of *TGFBR3* and *MGEA5* rearrangements can be applied as a reliable molecular test when confronted with limited biopsy material or a challenging diagnosis.

22 Loss of p16 Expression Differentiates Malignant Mesothelioma from Benign Mesothelial Proliferation.

H Aydin, D Chute, B Yang. Cleveland Clinic, OH.

Background: Although several antibodies relatively specific to mesothelial cells have been developed in discriminating mesothelial cells from adenocarcinoma, a few ancillary tools are available clinically to differentiate benign from malignant mesothelial proliferation. Recent molecular studies indicate that alteration of the p16 gene either by deletion or promoter hypermethylation is attributed to malignant transformation of mesothelial cells. However, difference on expression of p16 protein between benign and malignant mesothelial cells has not well investigated. We investigated the utility of p16 immunohistochemical staining in differentiating benign mesothelial proliferation from malignant mesothelioma.

Design: A total of 41 cases of mesothelial proliferation were retrospectively identified from our hospital archiving system, which include 10 cases of benign peritoneal multilocular mesothelial inclusion cysts (MMIC) and 31 cases of malignant mesothelioma. The latter encompasses 16 cases of surgically resected mesothelioma and 15 cases of cell blocks from pleural or peritoneal effusions. Expression of p16 was evaluated with p16 antibody kit (MTM, Germany) using the BenchmarkXT® instrument (Ventana Medical Systems, Inc., Tucson, AZ). Immunohistochemical staining pattern for p16 was evaluated with intensity (0, 1+, 2+ and 3+) and percentage of mesothelial cells.

Results: Among 10 cases of benign mesothelial proliferation (MMIC), strong (3+) and diffuse (>95% of cells) p16 immunoreactivity was seen in all the cases. In contrast, loss of p16 expression was seen in all 31 cases of malignant mesothelioma, including 80.7% (25/31) cases with total p16 negativity and 19.3% (6/31) cases with partial and weak p16 immunoreactivity (20-50% of cells). There is significant difference (p<0.001) of p16 immunoreactivity between benign mesothelial proliferation and malignant mesothelioma.

Conclusions: Overexpression of p16 protein is seen in benign multilocular mesothelial inclusion cysts. In contrast, loss of p16 protein is a hallmark of malignant mesothelioma cells. Immunohistochemical staining for p16 can be a useful ancillary tool in differentiating benign and malignant mesothelial proliferation.

23 Immunohistochemistry and Fluorescence In Situ Hybridization for INI1 in Proximal Type Epithelioid Sarcoma and Malignant Extrarenal Rhabdoid Tumor.

A Bahrami, S Raimondi, A Folpe. St. Jude Children's Research Hospital, Memphis, TN; Mayo Clinic, Rochester, MN.

Background: *INI1* is a tumor suppressor gene whose protein expression is known to be lost almost exclusively in certain tumors: epithelioid sarcomas (ES), malignant extrarenal rhabdoid tumors (MERT), and true rhabdoid tumors of central nervous system (ATRT) and kidney. Proximal-type ES (PTES) is a variant of ES with rhabdoid morphology, predilection for proximal extremities and more aggressive behavior than classical ES. Considerable debate exists as to whether PTES and MERT represent the same or different entities, and whether their frequency of *INI1* abnormalities differs.

We examined *INI1* alteration and INI1 protein loss in a group of such tumors with the goal of identifying distinct clinicopathologic characteristics between those with and without *INI1* aberrations.

Design: 8 cases previously coded as PTES, MERT, or ATRT were retrieved. All were immunostained for CK (OSCAR) and INI1, and a subset for CD34. FISH was conducted on FFPE tumor sections in all cases using a laboratory-developed dual-color probe containing INI1 [CTD-2511E13+CTD-2034E7](22q11.2) and PANX2 [RPCI3-402G11] (22q13.33) as control.

Results: Table 1 summarizes the clinical, immunohistochemical and FISH findings. Although all cases showed loss of INI1 expression by immunohistochemistry, FISH analysis showed only 2 cases with *INI1* deletion, 1 heterozygous and 1 homozygous. The ATRT was aneuploid for chromosome 22. There were no clinicopathologic features that distinguished cases with and without *INI1* deletion.

Table 1: Clinicopathologic, immunohistochemical and FISH findings

Case #	Age	Sex	Location	Pathology	CK AE1/3	CD34	INI1	FISH for INI1
1	21	M	RTP	PTES/MERT	+	NP	lost	Deletion (heterozygous)
2	56	M	RTP	PTES/MERT	+	NP	lost	No Deletion
3	58	M	Neck	PTES/MERT	+	-	lost	No Deletion
4	51	M	Chest/pleura	MERT	-	-	lost	No Deletion
5	60	F	Knee	PTES	+	+	lost	No Deletion
6	19	M	Knee	PTES	+	+	lost	No Deletion
7	44	F	Thigh	PTES/MERT	+	-	lost	Deletion (homozygous)
8	6	M	Bram	ATRT	NP	NP	lost	Aneuploidy for chr 22

RTP: retroperitoneum; Chr: chromosome; NP: Not performed

Conclusions: The rare finding of homozygous *INI1* deletion/mutation in our series supports the contention that other mechanisms, most likely through epigenetics and post-translational modifications, are responsible for suppression/inactivation of *INI1* gene production in most such cases. Although our sample size is too small to draw a definitive conclusion, our initial findings do not suggest any specific clinicopathologic features unique to *INI1* altered cases compared with those with only protein loss. The incidence of *INI1* alteration and its value as a reliable indicator for stratification of such cases into prognostically relevant categories should be evaluated in larger studies with clinical outcome data.

24 Expression of P16 in Osteosarcoma as Predictive Neo-Adjuvant Therapy Factor.

D Borys, RJ Canter, RM Tamurian, B Hoch, B Murphy, J Bishop, AE Horvai. University of California Davis, Sacramento; UC Davis, Sacramento, CA; University of Washington, Seattle; UCSF, San Francisco, CA; UC Davis, Davis, CA.

Background: Osteosarcoma is a common malignant primary tumor of bone affecting adolescent and young adults. Osteosarcomas are high grade sarcomas with aggressive behavior. There are few if any molecular markers to predict behavior and prognosis of osteosarcoma. The objective of this study is to investigate expression of p16 in correlation with neo-adjuvant chemotherapy response in osteosarcoma.

Design: A tissue micro array was created using paraffin embedded samples from 40 pretreatment osteosarcoma cases from two institutions UC Davis and UCSF. Immunohistochemistry was performed with commercially available p16 monoclonal mouse antibody (mtm laboratories AG, Germany). Expression of p16 was defined as cytoplasmic staining in at least 30% of cells. Percent tumor necrosis was measured in post-chemotherapy resection specimens with good response set at >90% necrosis. Data were also abstracted on age, sex, tumor site, and histologic subtype. Univariate and multivariate analysis was performed.

Results: Patients age ranged from 9 to 75 years (mean 20). Most common locations were tibia and femur. 21 patients were female and 19 male. The clinical and p16 results are summarized in [table 1]. p16 expression correlated positively with median percent necrosis and fraction of cases with good chemotherapy response (p=0.004 and 0.003, respectively). On multivariate analysis, p16 expression was independently associated with chemotherapy response after controlling for other factors.

TABLE 1. Comparison of Clinicopathologic Characteristics among p16 Over- and Under-Expressing Tumors

Characteristic	p16 Positive (N=25)	p16 Negative (N=15)	P Value
Median Age, IQR	15, 12-21	17, 13-26	0.51
Sex: Male/Female	15 (60%)/10 (40%)	4 (27%)/11 (73%)	0.06
Median Percent Necrosis/ Range	95/ 90-99	40/ 10-90	0.004
Pathologic "good" response (>90%)* : Yes/ No	18 (78%)/ 5 (22%)	4 (27%)/ 11 (73%)	0.003

*Indicates statistically significant difference

Conclusions: Immunohistochemical expression of p16 significantly correlates with chemotherapy response in osteosarcomas. p16 immunohistochemistry may be useful adjunctive marker of prognosis in osteosarcoma.

25 Tumor-Infiltrating Macrophages Are Associated with Metastasis Suppression in High-Grade Osteosarcoma: A Rationale for Treatment with Macrophage-Activating Agents.

EP Buddingh, ML Kuijjer, R Duim, H Burger, K Agelopoulos, O Myklebost, M Serra, F Mertens, PCW Hogendoorn, AC Lankester, A-M Cleton-Jansen. Leiden University Medical Center, Netherlands; University of Münster, Germany; The Norwegian Radium Hospital, Oslo University Hospital, Norway; Istituto Ortopedico Rizzoli, Bologna, Italy; Lund University Hospital, Lund, Sweden.

Background: High-grade osteosarcoma is a malignant primary bone tumor with a peak incidence in puberty. Overall survival of patients with resectable metastatic disease is approximately twenty percent. The exact mechanisms of development of metastases in osteosarcoma remain unclear. Most studies focus on tumor cells, but it is increasingly

evident that stroma plays an important role in tumorigenesis and metastasis. We investigated the development of metastasis using an integrative approach, in which both stroma and tumor cells were studied.

Design: To identify gene signatures playing a role in metastasis, we performed genome-wide gene expression profiling on pre-chemotherapy biopsies of patients who did (n=34) and patients who did not (n=19) develop metastases within five years. Immunohistochemistry was performed on pre-treatment biopsies from two additional cohorts (n=63 and n=16), and on corresponding post-chemotherapy resections and metastases.

Results: 118/132 differentially expressed genes were upregulated in patients without metastases. Remarkably, almost half of these upregulated genes had immunological functions, particularly related to macrophages. Macrophage-associated genes were expressed by infiltrating cells and not by osteosarcoma cells. Tumor-associated macrophages (TAMs) were quantified with immunohistochemistry and were associated with significantly better overall survival in the additional patient cohorts. Osteosarcoma samples contained both M1 (CD14/HLA-DR α positive) and M2 type TAMs (CD14/CD163 positive and association with angiogenesis).

Conclusions: In contrast to most other tumor types, TAMs are associated with reduced metastasis and improved survival in high-grade osteosarcoma. This study provides a biological rationale for the adjuvant treatment of high-grade osteosarcoma patients with macrophage-activating agents, such as muramyl tripeptide.

26 Primary Lymphoma of Bone (PLB): Lessons Learned from Radiological and Pathological Correlation.

MM Bui, J Caracciolo, N Riddle, W Bulkeley, L Zhang. Moffitt Cancer Center, Tampa; University of South Florida, Tampa.

Background: Adult PLB constitutes <1% of non-Hodgkin lymphoma. Because of its rarity and variable clinical and radiographic appearances, patients (pts) often seek initial care from the sarcoma service. However, due to the difference in the management of lymphoma versus sarcoma, it is critical to preoperatively recognize PLB. This study aims to identify the radiological characteristics of PLB and present a practical approach to aid in accurate diagnosis.

Design: A retrospective review of the pathology, radiology and clinical databases from our institution (1999-2009) was performed to identify pts with osseous lymphoma. PLB was defined as (a) a new, solitary bone lesion; (b) no known history of lymphoma; and (c) no evidence of systemic disease at diagnosis. Pathology and radiology data for initial diagnosis were correlated.

Results: Among 160 osseous lymphomas, 53 (33%) represented PLBs. Thirty-three pts had available radiological information. Preoperative differential diagnosis included lymphoma as a primary consideration in only 4 cases (12%). The most common differential diagnoses included metastasis (11) and "malignant or aggressive" (7). Findings on plain radiographs and CT were highly variable. Conversely, MRI revealed more specific findings including infiltrative medullary lesions with an associated extra-osseous mass and minimal cortical disruption relative to the size of the soft tissue component (14) and infiltrative medullary lesions without cortical destruction or an associated extra-osseous mass (9). Bone scans and/or PET scans were positive (12/12). Pathologic diagnosis included 23 (70%) diffuse large B-cell, 6 follicular and 4 other lymphomas. After on-site pathologic evaluation of biopsy and/or surgical specimens in 18 pts, lymphoma was included as a working diagnosis and the specimens were triaged for conformational ancillary studies. No on-site pathologic evaluation was done in 13 pts, which resulted in a second procedure/sampling for confirmation or subtyping.

Conclusions: PLB often presents with nonspecific clinical and imaging findings, thus not well recognized prior to intervention. MRI may provide the most specific imaging characteristics when compared to other imaging modalities. Given the much more common prevalence of other entities, radiologists should at least consider lymphoma in cases of solitary bone lesions, even if only to dismiss it in light of other clinical information. This will alert the pathologist to perform on-site evaluation of the fresh specimen and to triage appropriately for a timely and accurate final diagnosis.

27 Beta-Adrenergic Receptor Expression in Adult Vascular Tumors.

KM Chisholm, KW Chang, MT Truong, S Kwok, R West, AE Heerema-McKenney. Stanford University School of Medicine, CA; Cleveland Clinic, OH.

Background: Propranolol has been found to successfully cause regression in complicated infantile hemangiomas (IH). The B-adrenergic receptor antagonist is thought to lead to vasoconstriction by its downstream effect on nitric oxide, block angiogenesis by its downstream effect on vascular endothelial growth factor (VEGF), and lead to apoptosis. We recently reported expression of B-2 adrenergic receptor (B2-AR) its phosphorylated form (B2-ARP) in a case of IH responding to propranolol treatment (*J.Pediatr.* 156:335; 2010). We now explore the expression of B-adrenergic receptors on a variety of vascular lesions in adults utilizing a tissue microarray (TMA).

Design: A vascular tumor TMA containing 88 lesions (littoral cell angioma (7), epithelioid hemangioendothelioma (15), angiosarcoma (47), intimal sarcoma (5), Kaposi sarcoma (5), spindle cell hemangioma (5), and one case each of hemangioendothelioma of bone, retiform hemangioendothelioma, sinonasal hemangiopericytoma and lymphangioleiomyomatosis), was immunohistochemically stained for B2-AR, B2-ARP, and B3-AR, and scored for the intensity of endothelial cell expression as negative, weak positive or strong positive.

Results: Strong expression of B2-AR was consistently present in all cases of intimal sarcoma, spindle cell hemangioma and the bone hemangioendothelioma, as well as the majority of Kaposi sarcoma cases. Strong expression of B2-ARP was present in lymphangioleiomyomatosis, sinonasal hemangiopericytoma, retiform hemangioendothelioma, and in most Littoral cell angiomas and epithelioid hemangioendotheliomas. Strong expression of B3-AR was limited to most cases of epithelioid hemangioendothelioma and minority of cases of spindle cell hemangioma,

angiosarcoma, Kaposi sarcoma and intimal sarcoma. Strong expression of B2-AR and its phosphorylated form B2-ARP were not necessarily congruent, but weak expression of the counterpart was usually present.

Conclusions: This is the first study to report B-adrenergic receptor expression in a variety of adult vascular lesions. While immunohistochemical expression of these receptors does not necessarily indicate that similar pathways of responsiveness to beta-blockade are present in these lesions, their presence does raise the possibility that beta-blockade could potentially effect apoptosis and decreased responsiveness to VEGF. Additional study is warranted as therapeutic options are limited for many patients with these tumors.

28 Detection of MDM2 and CDK4 by Fluorescence In Situ Hybridization, Immunohistochemistry and Real-Time PCR in Liposarcoma: Prognostic Significance Based on the Molecular Diagnosis.

JH Cho, J Lee, SW Seo, JO Park, SJ Kim, G Ahn, Y-L Choi. Samsung Medical Center, Sungkyunkwan University School of Medicine, Seoul, Korea.

Background: The molecular characteristics have been useful in the grouping of liposarcoma. Especially, the amplification MDM2 and CDK4 is the main feature of well-differentiated liposarcomas (WDLs) and dedifferentiated liposarcomas (DDLs). Even though MDM2 and CDK4 are coamplified in most cases, the detailed status has not been elucidated. The aim of this study was to assess the clinical significance based on the status of molecular diagnosis, especially MDM2 and CDK4 amplification.

Design: Eighty three cases of liposarcomas and sixty cases of lipomas diagnosed between 1995 and 2007 were analyzed for the presence of MDM2 amplification using fluorescence in situ hybridization (FISH). MDM2 and CDK4 level also investigated by real-time quantitative PCR (QPCR) and immunohistochemistry. The subtype of liposarcoma was re-classified depending on the results of molecular status. Disease free survival (DFS) and overall survival (OS) were estimated with the Kaplan-Meier method and compared with the log rank test based on the previous histology and re-classified molecular diagnosis.

Results: FISH and QPCR showed highly concordant results. Among 60 lipomas, one case was reclassified as WDL. Three myxoid liposarcomas were reclassified as DDLs and three WDLs as lipomas. The re-classified 79 cases were divided into 38 WDLs, 15 DDLs, 7 pleomorphic liposarcomas (PLs), and 19 myxoid/round cell liposarcomas. Three cases out of 60 MDM2-amplified liposarcomas showed no amplification of CDK4 by QPCR. MDM2 polysomy was detected in FISH and QPCR, especially in the cases of DDLs and PLs. Molecular classification showed better discrimination for the DFS and OS. In the MDM2/CDK4-amplified liposarcomas, CDK4 QPCR level was a significant prognostic factor for DFS but not MDM2 QPCR level.

Conclusions: The use of molecular testing by FISH or QPCR of lipomatous tumors is important to compromise the histology and IHC for the precise grouping of the disease and prediction of the prognosis.

29 Primary Retroperitoneal Liposarcomas: Mitoses in Non-Adipogenic Zones Correlate with Survival.

S Chopra, Y Li, D Gui, FC Eilber, SM Dry. UCLA, Los Angeles, CA; Tata Medical Center, Kolkata, India.

Background: Non-lipogenic areas are considered evidence for dedifferentiation in liposarcomas. The significance of low grade histology in non-lipogenic areas has been controversial. We evaluated a series of retroperitoneal lipomatous tumors with primary resection at UCLA and compared histologic features with outcome.

Design: Forty-six retroperitoneal liposarcomas with clinical follow up were identified in our database. Slides were evaluated for: 1. extensive non-lipogenic areas (ExNLA) (defined as bands at least as wide as a 10X field and overall occupying 50%+ of at least one slide), 2. hypercellularity (defined as overlapping nuclei) within non-lipogenic regions and 3. maximal mitoses in 10 HPFs, with at least 50 fields counted. Cases were stratified into two groups based on cellularity: well-differentiated liposarcomas (WDL), +/- ExNLA with normocellularity (N=7) and liposarcomas +/- ExNLA with at least focal hypercellularity (N=39). The hypercellular group was subdivided into tumors with 0-4 mitoses/10 hpfs (LS0-4) (N=19) and tumors with ≥5 mitoses/10 hpfs (N=20) (LS5+). Histologic data was correlated with patient status, length of follow up and time to recurrence in all cases.

Results: Kaplan-Meier disease specific survival analysis demonstrates a statistically significant difference in survival between the LS0-4 and LS5+ groups (p=0.02). Fourteen patients died of disease (2/7 in WDL, 3/19 in LS0-4 and 9/20 in LS5+). 18 patients experienced 22 local and 1 distant (lung) recurrences (2/7 patients in WDL, 8/19 in LS0-4 and 13/20 in LS5+). Two recurrences occurred in 3 patients (1 LS0-4 and 2 LS5+) and 3 recurrences in one patient (LS0-4). One WDL transformed to LS5+ in a recurrence; no pathology was available for recurrences in 1 WDL and 3 LS0-4. ExNLA was seen in 2/7 WDL, 17/19 LS0-4 and all LS5+; the WDL were normocellular with rare mitoses (0-3/10). Kaplan-Meier analysis did not show significant survival differences between the WDL and LS0-4 groups, but analysis was limited by short follow up time in several members of the small WDL group.

Conclusions: Most (39/47, 83%) retroperitoneal liposarcomas in our series show ExNLA with or without hypercellularity. Importantly, liposarcomas with ExNLA and 5+ mitoses per 10 HPFs have statistically significant shorter survival than tumors with 0-4 mitoses. These results suggest the term "dedifferentiated" may be more appropriate for LS5+ cases only, while LS0-4 cases may be better termed "well-differentiated liposarcoma with increased cellularity".

30 Oncofetal Protein IMP3: A Specific Biomarker That Distinguishes Leiomyoma from Leiomyosarcoma.

K Cornejo, M Shi, Z Jiang. UMass Memorial Medical Center and University of Massachusetts Medical School, Worcester.

Background: The diagnosis of leiomyosarcoma can be very difficult when distinguishing these lesions from variants of leiomyoma. IMP3, an oncofetal protein plays an important role in embryogenesis and carcinogenesis of certain malignant neoplasms. Several studies have shown that IMP3 is a cancer specific biomarker. The aim of this study was to investigate the expression of IMP3 in leiomyoma and leiomyosarcoma and to determine whether IMP3 can serve as a diagnostic biomarker for leiomyosarcoma.

Design: A total of 146 cases (resection, n= 118; biopsy, n=28) obtained from the surgical pathology files of a tertiary Medical Center consisting of 62 leiomyomas (uterine, n=59; soft tissue, n=2) and 84 leiomyosarcomas (uterine, n=15; soft tissue, n=69) were examined by immunohistochemistry for IMP3 expression. Among the leiomyosarcoma cases, 54 were primary, and 30 were metastatic. All cases were collected between January 1997 and December 2009, and the diagnosis was confirmed by at least two pathologists.

Results: A positive immunohistochemical stain for IMP3 (cytoplasmic staining) was not identified in any of the 62 leiomyoma cases (0%) and was significantly increased (p<0.0001) in leiomyosarcoma highlighting 43 of 84 cases (51%). Of the 84 leiomyosarcoma cases, 54 were primary and 30 were metastatic with IMP3 staining in 50% and 53% of cases, respectively. IMP3 positivity was detected in >50% of tumor cells in 19 (23%) cases, 26-50% of tumor cells in 9 (11%) cases and <25% of tumor cells in 15 (18%) cases. IMP3 expression was detected in 23 of 44 (52%) intermediate and high-grade (nuclear grade II-III/III) and 4 of 7 (57%) low-grade leiomyosarcomas (nuclear grade I/III). Positive IMP3 staining was detected within 7 of the 15 (47%) cases of uterine and 36 of the 69 (52%) cases of soft tissue leiomyosarcomas. The sensitivity of IMP3 for the detection of leiomyosarcoma was 51% and the specificity was 100%.

Conclusions: The high degree of specificity of IMP3 for leiomyosarcoma suggests it can be used as a diagnostic biomarker. The expression of IMP3 in tumor cells can increase the level of confidence in establishing a definitive malignant diagnosis in both uterine and soft tissue leiomyosarcomas.

31 Detection of MDM2/CDK4 Amplification in Lipomatous Soft Tissue Tumors from Formalin-Fixed, Paraffin-Embedded Tissue: Comparison of Multiplex Ligation-Dependent Probe Amplification (MLPA) and Fluorescence In Situ Hybridization (FISH).

D Creyten, S Ah Schoondermark-Stolk, E-J Speel, J van Gorp, P Pauwels. University Hospital Antwerp, Antwerp, Belgium; Diaconessen Hospital Utrecht, Utrecht, Netherlands; University Hospital Maastricht, Netherlands.

Background: Several recent publications show that atypical lipomatous tumors (ALT)/well-differentiated liposarcomas (WDLPS) and dedifferentiated liposarcomas (DDLPS) share common molecular cytogenetic abnormalities, such as the presence of ring or large-marker chromosome containing amplification of the 12q14-15 region, including the MDM2 and CDK4 genes. Recently, a new method has been described for the measurement of gene copy number: MLPA.

Design: In this study the detection of MDM2 and CDK4 amplification was evaluated in lipomatous soft tissue tumors using MLPA, a PCR based technique, in comparison with FISH on a series of 85 formalin fixed paraffin embedded lipomatous tumors (27 benign adipose tumors, 36 ALT/WDLPS, 18 DDLPS, and 4 pleiomorphic liposarcomas (PLPS) to identify amplification of MDM2 and CDK4 genes and compared the results with those obtained with FISH and MDM2/CDK4 immunohistochemistry.

Results: No amplification was seen in the benign adipose tumors and PLPS. MDM2 and CDK4 immunoeexpression was seen in 4 and 2 benign adipose tumors respectively. Amplification was detected in 16 and 20 of the 32 ALT/WDLPS by MLPA and FISH respectively. In 2 of the MDM2 amplified cases there was no amplification of CDK4. MDM2 and CDK4 immunoeexpression was seen in 32 and 30 ALT/WDLPS respectively. 4 cases of a ALT/WDLPS with a low amplification level (ratio ranging between 2 and 2,3) detected by FISH were undetected by MLPA. In 12 of the 16 DDLPS amplification was detected by MLPA and FISH. MDM2 and CDK4 immunoeexpression was seen in 16 and 15 DDLPS respectively.

Conclusions: The concordance between MLPA and FISH was 100% in cases of a high level of amplification of MDM2 and CDK4. A few cases of a ALT/WDLPS with a low amplification level detected by FISH were undetected by MLPA. Therefore, MLPA proves to be an appropriate technique for screening MDM2/CDK4 amplification in lipomatous soft tissue tumors, which provides an alternative or additional test to determine MDM2 and CDK4 amplification in liposarcomas. Surprisingly was that 12 of 32 cases of ALT/WDLPS showed no MDM2 and CDK4 amplification by FISH and MLPA. All these 12 cases were relatively small and all subcutaneous. These cases were revised and are morphologically and immunohistochemically not different from ALT with MDM2/CDK4 amplification.

32 Pigmented Villonodular Synovitis (PVNS): More Prevalent Than Previously Reported.

TM D'Alfonso, MJ Klein, EF DiCarlo. Weill Cornell Medical College, New York, NY; Hospital for Special Surgery, New York, NY.

Background: Pigmented villonodular synovitis (PVNS) is a benign but locally aggressive tumor affecting the synovium, tendon sheaths, and bursae. In the literature, PVNS is regarded as a rare process with a reported incidence of 1.8 cases per million (0.000018%) in the general population. Based upon our experience at a large referral center, we believe that PVNS is more common, particularly in the knee, than has been reported, prompting this current study. Here we report the results of a retrospective

analysis of all cases of PVNS diagnosed at our institution over a 15 year period.

Design: All cases of PVNS identified from our files from 1995 to 2010 were included in the study. Tumors were classified as "incidental" if they were discovered in specimens from procedures performed on patients for a pre-operative diagnosis other than PVNS, e.g. degenerative joint disease (DJD), or if the pathologist had specifically documented the tumor as incidental in the report. Estimated prevalence of PVNS in the knee was calculated by dividing the number of incidental cases of PVNS by the total number of knee replacements performed over the same time period.

Results: 32,206 patients underwent total knee replacement surgery during the study period. 317 of these patients were diagnosed with PVNS, with PVNS an incidental finding in 110 of these cases. From this information, we estimate the prevalence of PVNS in patients undergoing total knee replacement to be between 0.3 and 0.9%.

Conclusions: In prior studies, the incidence of PVNS was established based on cases in which PVNS was the targeted lesion. In our study we calculated prevalence based on incidental PVNS discovered in patients with unrelated knee disease, predominantly DJD. We found PVNS to be far more prevalent in patients undergoing surgery for reasons other than PVNS, suggesting that the actual prevalence of PVNS in the general population is likely significantly higher than what has been previously reported.

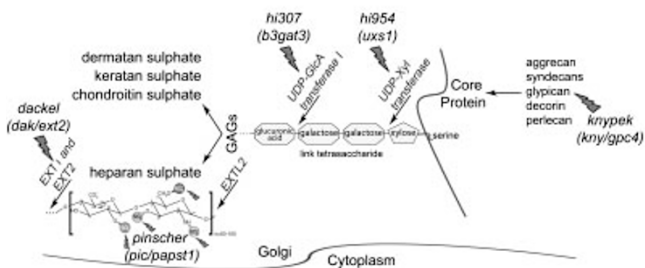
33 The Pathogenesis of Osteochondroma: Clues from Tracing Proteoglycans in Zebrafish Models and Human Cartilage.

CE de Andrea, MI Wiveger, FA Prins, PCW Hogendoorn. Leiden University Medical Center, Netherlands.

Background: Proteoglycans (PGs) are extracellular modulators of protein gradient formation. In cartilage, the gradient of heparan sulfate PGs can either regulate endochondral ossification in the growth plate or, when disrupted, originate osteochondroma, the most common bone tumor at adolescences. PGs may be traced electron microscopically by polyethyleneimine (PEI), which binds their negatively charged sites, providing insights into tumor formation.

Design: Pre-embedding PEI was studied by electron- and reflection contrast microscopy in human growth plate, osteochondroma and five different proteoglycan-deficient zebrafish. *dackel* (*dak;ext2*) mutant, a fish homologue of human multiple osteochondromas, has decreased levels of heparan sulfate; *hi307* (*β3gat3*) has reduced heparan and chondroitin sulfates; *hi954* (*uxs1*) has impaired PGs biosynthesis; *pinscher* (*pic;papst1*) lacks sulfate groups; and *knypek* (*kny;gpc4*) lacks Glypican-4. Matrix formation was analyzed using the plot profile tool of ImageJ software.

Five lines of homozygous zebrafish mutants (in *italics*) with different defects in proteoglycans biosynthesis used in the present study.



Results: Electron-dense deposits of PEI were observed within the extracellular matrix of the human growth plate and wild-type zebrafish cartilage. In both instances, the plot profile showed gradient formation, in which the size and number of PEI aggregates decreased with the distance from the cell surface. A similar pattern was found in the *hi307* and *kny* mutants. In the *pic* and *hi954* mutants, no PEI aggregates were identified. In *dak*, a prominent reduction of PEI and no gradient formation were observed. In osteochondroma the majority of the chondrocytes established a normal gradient. However, 10% of the osteochondroma cells resembled *dak*-chondrocytes. The matrix surrounding these cells were virtually free of PEI and gradient reflecting areas inside the tumor where cell-cell interactions might be impaired by the reduction of PGs especially heparan sulfate.

Conclusions: Pre-embedding PEI in cartilage provides a significant advance towards the regulation of growth plate and the pathogenesis of osteochondroma and leads to the hypotheses: 1. Osteochondroma is a mosaic of normal and PGs deficient cells. 2. Growth plate chondrocytes harboring homozygous mutation in *EXT1/2* genes might disrupt the diffusion gradients and signal transduction initiating tumor formation.

34 Activation of the PI-3-Kinase Pathway and Prognostic Factors in Myxoid Liposarcoma.

EG Demicco, KE Torres, M Ghadimi, C Columbo, T Peng, D Lev, W-L Wang, AJ Lazar. The University of Texas M.D. Anderson Cancer Center, Houston.

Background: Myxoid liposarcoma (MLPS) is a common liposarcoma subtype. Hypercellularity evidenced by diffuse round cell (RC) change predicts a more aggressive clinical course. Recently, several biomarkers have been proposed to have prognostic significance in MLPS, including Ki-67 and p53. It has also been shown that PI3KCA is mutated in 18% of MLPS resulting in activation of the PI3K/Akt pathway and poor prognosis. As this event represents a therapeutic target, we evaluated expression of phosphorylated downstream targets of the PI3K/Akt pathway (p6SRP and pEBP1) in a large series of MLPS with clinical follow-up to investigate the prevalence of activation of this pathway by mutation or other avenues.

Design: From our institutional prospective MPLS clinical database of 403 patients, 170 specimens from 111 patients with FFPE tissue were retrieved and formatted into a tissue microarray. Immunohistochemistry for Ki-67, p53, p6SRP and pEBP1 was performed and tabulated with clinicopathologic details.

Results: The studied patient population (n=111) included 68 men and 43 women, with an age range of 17 – 79 years (median, 42). Primary sites included: lower extremity (78%), trunk (20%), and upper extremity (2%). Metastases evolved in 53 patients, sites included: retroperitoneum (42%), lung (21%), chest wall (21%), spine (11%), and flank (6%).

The TMA included 74 primaries, 60 metastases, and 24 recurrent tumors. 50 tumors showed histologic evidence of prior chemo- or radio-therapy. Nuclear Ki-67 expression was elevated ($\geq 10\%$) in 20% of conventional MLPS and 39% of cellular/RC MLPS ($p = 0.05$), while nuclear p53 was overexpressed in 21% and 41% of these two groups, respectively ($p = 0.05$). Treated tumors had uniformly low Ki-67. Activation of the PI3K/Akt pathway was confirmed by immunoreactivity for p6SRP and pEBP1 in 55% and 62% of all cases, respectively. High expression of p6SRP was seen in 45% of conventional MLPS, 44% of cellular MLPS, and 84% of treated cases, while pEBP1 expression trended to association with cellular MLPS (81%), vs conventional (60%, $p = 0.074$) or treated (46%).

Conclusions: Expression of both Ki-67 and p53 correlated with aggressive histology. Significant expression of both p6SRP and pEBP1 confirmed activation of the PI3K/Akt pathway, where multiple inhibitors are in clinical trials, although p6SRP was not associated with aggressive histologic features. PI3KCA genotyping and correlation of biomarkers with clinical outcome in a multivariate analysis is ongoing.

35 The Hemangiopericytoma/Solitary Fibrous Tumor Spectrum: Clinicopathologic Predictors of Outcome.

EG Demicco, MS Park, DM Araujo, AJ Lazar, W-L Wang. The University of Texas M. D. Anderson Cancer Center, Houston.

Background: Hemangiopericytoma (HPC) / Solitary fibrous tumor (SFT) represents a spectrum of uncommon mesenchymal tumors of uncertain malignant potential. Classic histologic determinants of behavior include: cellularity, mitotic activity, and foci of hemorrhage and necrosis. We evaluated these features in prediction of local recurrence or metastasis in a series of HPC/SFT with clinical follow-up.

Design: Our institutional database identified 553 patients with HPC/SFT. Of these, 130 adult patients with complete clinical follow-up were included. The features of primary meningeal and sinonasal HPC are well-described; these cases were excluded from histologic analysis. Of the remaining cases, 28 primary resection specimens were available for histologic review

Results: The initial study patient population (n= 130), included 71 men and 59 women, with an age range of 15-88 yrs (median, 54). Primary tumor sites included CNS/meninges (27%), abdomen/pelvis (23%), lung/pleura (13%), head/neck (17%), and extremities (17%). At presentation to our institution, 54% had primary resectable disease, while 46% had unresectable, locally advanced disease or metastases, likely due to referral bias. Cases available for histologic review included 15 women and 13 men. Tumor size averaged 13.8 cm (range: 2-23.5). Following surgical resection, 11 patients experienced recurrence with a median of 37 mo (range: 7-163), either locally only (n=4), with distant metastases only (n=5), to lung/pleura, bone, abdomen or liver, or with both local and distant disease (n = 2). Of these patients, 9 died of disease.

Tumor recurrence (local or metastatic) was associated with older age at presentation (mean age 63 vs. 48; $p = 0.009$), larger tumor size ($20 \text{ cm} \pm 8.2$ vs. $8.8 \text{ cm} \pm 4.2$; $p < 0.0001$), and increased mitotic rates (mean: 8/10 HPF vs 2/10; $p = 0.01$). No significant differences in cellularity, nuclear pleomorphism or necrosis/hemorrhage were observed. Marked pleomorphism was seen focally in 3 cases, of which 2 had poor outcomes.

Conclusions: We report the preliminary results of our institutional experience with HPC/SFT. Of the classic histologic determinants in HPC/SFT, in our patient population, only mitotic activity and tumor size showed prognostic power. Negative indicators included age ≥ 60 , increased size (≥ 10 cm), and elevated mitotic count ($> 2/10$ HPF). Additional studies are ongoing.

36 MUC4 is a Highly Sensitive and Specific Marker for Low-Grade Fibromyxoid Sarcoma.

LA Doyle, E Moller, F Mertens, JL Hornick. Brigham and Women's Hospital, Boston, MA; Lund University Hospital, Lund, Sweden.

Background: Low-grade fibromyxoid sarcoma (LGFMS) is a distinctive fibroblastic neoplasm characterized by alternating collagenous and myxoid areas, deceptively bland spindle cell morphology, a whorling architecture, and a t(7;16) translocation involving FUS and CREB3L2. Owing to variable morphology and a lack of discriminatory markers, LGFMS can be difficult to distinguish from benign mesenchymal tumors and other low grade sarcomas. Global gene expression profiling has identified differential expression of the mucin 4 (MUC4) gene in LGFMS compared to histologically similar tumors. MUC4 is a transmembrane glycoprotein that functions in cell growth signaling pathways; aberrant MUC4 expression has been reported in various carcinomas. We investigated MUC4 protein expression by immunohistochemistry (IHC) in a well-characterized series of LGFMS and other soft tissue tumors to determine the potential diagnostic utility of this novel marker.

Design: Whole tissue sections of 286 tumors were evaluated: 44 LGFMS (all with FUS rearrangement confirmed by FISH), 40 soft tissue perineuromas, 22 myxofibrosarcomas (12 low, 6 intermediate, 4 high grade), 20 cellular myxomas, 20 solitary fibrous tumors, 20 low-grade malignant peripheral nerve sheath tumors, 20 desmoid fibromatosis, 20 neurofibromas, 20 schwannomas, 20 monophasic synovial sarcomas [all confirmed to harbor t(X;18)], 20 dermatofibrosarcoma protuberans, 10 myxoid liposarcomas, and 10 extraskelletal myxoid chondrosarcomas. IHC was performed following pressure cooker antigen retrieval using a mouse anti-MUC4 monoclonal antibody (1:500; 8G7;

Santa Cruz). The extent of immunoreactivity was graded according to the percentage of positive tumor cells (0, no staining; 1+, <5%; 2+, 5-25%; 3+, 26-50%; 4+, 51-75%; and 5+, 76-100%).

Results: The LGFMS cases included 6 with marked hypercellularity, 4 with prominent HPC-like vessels, 3 with giant collagen rosettes, 3 with epithelioid morphology, 2 with focal nuclear pleomorphism, and 2 with areas of sclerosing epithelioid fibrosarcoma. All 44 LGFMS cases (100%) showed cytoplasmic staining for MUC4, which was usually diffuse and intense (5+ in 42 cases; 4+ in 1; 3+ in 1). All other tumor types were negative for MUC4, apart from focal reactivity in 6 (30%) monophasic synovial sarcomas and 1 (2%) soft tissue perineurioma.

Conclusions: MUC4 is a highly sensitive and specific IHC marker for LGFMS and can be helpful to distinguish this tumor type from histologic mimics. Expression of MUC4 in other soft tissue tumors is very limited in distribution.

37 ROR2: A Potential Therapeutic Target in Soft Tissue Tumors.

B Edris, I Espinosa, AH Beck, C-H Lee, AJ Lazar, D Lev, JA Fletcher, RB West, R Nusse, M van de Rijn. Stanford University School of Medicine, CA; Universitat Autònoma de Barcelona, Spain; Vancouver General Hospital, BC, Canada; MD Anderson Cancer Center, Houston, TX; Harvard Medical School, Boston, MA.

Background: Receptor tyrosine kinases (RTKs) are a family of cell surface receptors that regulate a range of normal cellular processes and that can play critical roles in cancer development and progression. Receptor Tyrosine Kinase-Like Orphan Receptor 2 (ROR2) is activated by its ligand Wnt5A during the course of normal bone and cartilage development. ROR2 has been shown to have pro-tumorigenic effects in osteosarcoma, renal cell carcinoma, and melanoma. However, the prognostic significance of ROR2 expression in mesenchymal tumors has yet to be shown.

Design: Gene expression profiling data from a series of soft tissue tumors were analyzed for ROR2 gene expression. Next, we performed an immunohistochemistry analysis using a novel ROR2 antibody on tissue microarrays that contained leiomyosarcoma (LMS), gastrointestinal stromal tumor (GIST), and desmoid-type fibromatosis (DTF) tumors with known clinical outcome. To interrogate the functional significance of ROR2 expression in tumor proliferation and metastasis, we performed *in vitro* cell proliferation and matrigel invasion assays with LMS cells using small interfering RNAs to down-regulate ROR2 expression.

Results: Gene expression profiling revealed high levels of ROR2 mRNA expression in a subset of LMS, GIST, and DTF samples. These finds were confirmed by ROR2 immunostaining of tissue arrays containing 147 primary LMS, 417 GIST, and 195 DTF tumors. Kaplan-Meier survival curve analysis showed that high expression of ROR2 was associated with poor patient outcome in LMS ($p=0.017$) and GIST ($p=0.039$) but no statistical significance was reached in DTF. *In vitro* experiments demonstrated that reductions in ROR2 expression levels did not affect the proliferative capacity of LMS cells but did decrease their ability to invade through a matrigel matrix.

Conclusions: ROR2 is highly expressed in a subset of LMS, GIST, and DTF cases and high ROR2 protein expression is significantly associated with poor clinical outcome in patients with LMS and GIST. ROR2 expression is important for LMS cells to successfully migrate through a matrigel matrix, which implies an important role for ROR2 in mediating invasive ability. Taken together, these results suggest that ROR2 may represent a novel therapeutic target for the treatment of GIST, LMS, and possibly DTF.

38 The Non-Diagnostic Needle Core Biopsy in Musculoskeletal Pathology.

CD Elliot, B Chow, DDJ Howarth, RA Kandel, BC Dickson. Mount Sinai Hospital, Toronto, ON, Canada.

Background: Needle core biopsy represents a safe, efficient and accurate technique in the diagnosis of tumors arising in the bone and soft tissues. While much has been published on this topic, guidelines on re-sampling in the event of a non-diagnostic sample are lacking.

Design: We performed a retrospective review of our pathology archives for all needle core biopsies performed on lesions arising in the bone or soft tissues (2005-2009).

Results: A total of 1004 needle core biopsies of the bone and soft tissue were identified. Of these cases a total of 56 (5.6%) were deemed to be diagnostically insufficient (9 bone, 8 joint and 39 soft tissue). 32 patients underwent a second biopsy in the form of either a repeat needle core biopsy (7) or an open biopsy (25) as part of their management. All of the cases followed by an open biopsy (100%) resulted in a diagnosis. Five of the repeat needle core biopsies were diagnostic (71.4%), while two were not (28.6%). For those with a diagnosis, the cases included: 6 malignant and 5 benign soft tissue neoplasms, 5 vascular lesions, 5 lymphoid neoplasms, 3 giant cell tumors, 2 osteosarcomas, 1 osteomyelitis, 1 ganglion cyst and a case each of metastatic melanoma and carcinoma.

Conclusions: This study reaffirms the utility of the needle core biopsy in the diagnosis of musculoskeletal lesions. Our percentage of non-diagnostic cases is similar to that of published reports. In the majority of instances inadequate sampling appears to be the cause of diagnostic insufficiency; however, in retrospect, potential diagnostic clues could be identified in a minority of cases. It is interesting that a greater percentage of non-diagnostic cases appear to occur with lymphoid and vascular lesions. It is possible that lymphoid proliferations are over-represented in our sample population; as well, a greater amount of lesional tissue may be necessary for ancillary studies to facilitate a diagnosis. Vascular lesions were less common in our dataset and it is unclear if lesion heterogeneity contributed to a greater percentage of insufficient cases. In the event of a negative core biopsy an open biopsy remains the most reliable means of securing a diagnosis. Nevertheless, a repeat needle core often yields a diagnostic specimen and may have a role in some clinical situations.

39 Fusion of Non-Muscle Myosin MYH9 to the USP6Oncogene in Nodular Fasciitis.

MR Erickson-Johnson, MM Chou, BR Evers, CW Roth, AR Seys, L Jin, X Wang, Y Ye, AW Lau, AM Oliveira. University of Pennsylvania School of Medicine, Philadelphia; Mayo Clinic, Rochester, MN.

Background: Nodular fasciitis (NF) is a self limited mesenchymal lesion of uncertain etiology that commonly affects younger individuals. Rapid growth, rich cellularity and brisk mitotic activity often lead to a misdiagnosis of sarcoma. Only rare putative cases of NF have been characterized at the cytogenetic level but no consistent anomaly has been identified. While studying the biology of the *USP6* oncogene, we observed that subcutaneous xenografts of MC3T3 pre-osteoblasts overexpressing *USP6* produced lesions with clinical and histologic features similar to human NF. These observations led us to investigate whether *USP6* transcriptional upregulation could be involved in the pathogenesis of NF arising in humans.

Design: Stable cell lines expressing *USP6* were generated in MC3T3-E1 pre-osteoblasts and injected into nude mice. Two frozen samples and 13 additional paraffin-embedded tissues from classic examples of human NF were retrieved from the Mayo Clinic tumor archives (n=15). *USP6* mRNA expression profile was performed using semi-quantitative RT-PCR. Fusion gene identification was carried out using 5' RACE RT-PCR. Fluorescence *in situ* hybridization (FISH) was performed for the following loci: *USP6*, *CDH11*, *COL1A1* and *MYH9*. Confirmatory specific RT-PCR and direct sequencing for *MYH9-USP6* was performed in all 15 cases and 16 non-NF controls.

Results: Xenograph-induced tumors showed clinico-pathologic features similar to those seen in human NF. *USP6* mRNA transcriptional upregulation was identified in the two index cases of human NF. FISH analysis showed a balanced rearrangement of the *USP6* locus in 14 of 15 human NF cases (93%). 5' RACE, RT-PCR and direct sequencing identified the fusion of *MYH9* exon 1 to either exon 1 or 2 of *USP6*. *MYH9* locus rearrangement was found in 13/15 (87%) of the NF cases. One case showed rearrangement of *USP6* only (without *MYH9*), and one case showed no rearrangement of either gene. No rearrangement of *COL1A1* or *CDH11* was found. RT-PCR and sequencing confirmed the fusion *MYH9-USP6* in 11 of 15 NF (73%). Non-NF tumors were negative for *MYH9-USP6* fusion.

Conclusions: Our study provides new insight into the biology of NF, which can be viewed as a self-limited form of neoplasia. The mechanism seems to involve *USP6* transcriptional upregulation due to its fusion with a strong ectopic promoter, akin to what was seen previously in aneurysmal bone cyst. The identification of a sensitive and specific abnormality in NF may also provide a novel diagnostic avenue for these lesions.

40 CSF1-Response Signature Is Associated with Tumor Angiogenesis in Non-Gynecological Leiomyosarcoma.

I Espinosa, A Beck, B Edris, C-H Lee, R West, M van de Rijn. Stanford University School of Medicine, CA; Universidad Autònoma de Barcelona, Spain; University of British Columbia, Vancouver, Canada.

Background: Both Colony-Stimulating Factor-1 (CSF1) expression by tumor cells and stromal macrophage infiltration are associated with poor prognosis in leiomyosarcoma (LMS) but the mechanisms underlying these observed prognostic associations are not well understood. While it has been shown that in carcinomas, tumor-associated macrophages (TAMs) have been found to promote tumor angiogenesis, no such relationship has been exhibited in LMS.

Design: We analyzed the relationship between genes we previously identified to correlate with macrophage-rich inflammatory infiltration in tumor sites ("CSF1 Signature") with genes that play key roles in angiogenesis; this analysis was carried out in a series of LMS cases for which we had gene expression profiling data. We subsequently examined the density of CD34-positive microvessels in relation to *CSF1* expression, VEGFC expression, macrophage density, and patient outcome in a series of 76 gynecologic and 73 non-gynecologic primary LMS.

Results: VEGFC and vascular markers like CD34 were found to be positively associated with the CSF1 Signature in non-gynecologic LMS. VEGFA and VEGFB showed no association with CSF1 levels. On average, gynecologic LMS showed greater microvessel density (35/0.6mm) than non-gynecologic LMS (22/0.6mm) ($P<0.05$). For non-gynecologic LMS, microvessel density correlated with *CSF1* expression, macrophage density, and VEGFC expression (all with $P<0.05$). The presence of increased microvessel density was associated with decreased disease-specific survival by Kaplan-Meier analysis ($P=0.004$), while no correlation was found between vessel density and VEGFC levels. There was no significant correlation between microvessel density and patient survival in gynecologic LMS. The patterns of *CSF1* expression, macrophage recruitment and microvessel density were well maintained between primary-metastatic tumor pairs indicating that these features are intrinsic to the biology of LMS.

Conclusions: These findings link increased microvessel formation to tumoral *CSF1* expression and stromal macrophage infiltration and suggest enhanced tumor angiogenesis as a mechanism utilized by CSF1-recruited/activated stromal macrophages to aid the progression of non-gynecologic LMS.

41 FAP-Associated Desmoid Fibromatosis: A Comparison to Their Sporadic Counterparts.

WC Foo, C Colombo, D Whitting, S Hajibashi, W-L Wang, D Lev, AJ Lazar. The University of Texas, M.D. Anderson Cancer Center, Houston.

Background: Desmoid fibromatosis (DF) is fibroblastic/myofibroblastic neoplasm. Most arise sporadically with β -catenin (CTNNB1) mutations, but some are associated with familial adenomatous polyposis (FAP) having mutations in the adenomatous

polyposis coli (APC) gene. We reviewed the clinical features of FAP-DF and examined immunoreactivity with a select panel in FAP-DF, compared the two populations, and correlated these biomarkers with clinical behavior.

Design: From our database of 613 DFs, 51 clinically and/or molecularly confirmed FAP-DFs were found with FFPE tissue (25 available). They were formatted to a tissue microarray (TMA) and evaluated for their expression of β -catenin, cyclin D1, p53, and MIB-1. β -catenin staining was evaluated for nuclear and cytoplasmic intensity and distribution. For cyclin D1, p53, and MIB-1, percentage of nuclear staining was recorded. The results were compared to a previously characterized TMA of sporadic DF (213 specimens).

Results: FAP-DF showed nuclear staining for β -catenin (30%-90%; median, 80%; intensity: 10 high, 7 low; 8 core needle biopsies were excluded, see below). All 20 evaluable FAP-DFs showed both cyclin D1 (1%-20%; median, 5%) and p53 immunoreactivity (1%-60%; median, 20%). 16/21 evaluable FAP-DFs showed MIB-1 immunoreactivity (1%-5%; median 1%). For β -catenin staining, there was no statistically significant difference between sporadic and FAP-DF. There was significantly increased cyclin D1 ($p < 0.0001$) and p53 ($p < 0.05$) staining in FAP-DF. Clinically, 40/51 FAP patients had intrabdominal/abdominal wall DF that arose within a median of 3 years in the area of prior colonic surgery. 10 patients had extra-abdominal tumors unrelated to a surgical site. 18 patients had multiple DFs involving distinct sites.

Conclusions: While β -catenin levels were similar despite the known genetic differences in FAP-DFs and sporadic DFs, nuclear cyclin D1 encoded by a target gene of β -catenin and p53 (believed to be modulated by β -catenin signaling) are increased perhaps providing insight into molecular pathogenesis. This study underscores the usefulness of nuclear β -catenin immunoreactivity specifically in FAP-DF, as is now well-established for sporadic DF. In our experience, for reasons unclear, nuclear β -catenin immunoreactivity is often reduced or absent in needle biopsies (both sporadic and FAP-DF compared to resections), and represents an important false negative and potential diagnostic pitfall.

42 Myxoid Liposarcoma: A Clinicopathologic Study of 27 Cases of Primary Untreated Disease with Particular Focus on So-Called Transitional and Round Cell Areas.

KJ Fritchie, D Wang, JR Goldblum, SA Lietman, J Bodo, SD Billings, BP Rubin. Cleveland Clinic, OH.

Background: Data suggest that round cell areas in myxoid liposarcoma (MLS) correlate with an adverse outcome, but there has been variability in the definition of round cell liposarcoma (RCLS). Very little attention has been paid to so-called transitional areas (TLS), and the impact of TLS on prognosis is not well studied.

Design: 27 cases of primary, untreated MLS were evaluated using a semi-quantitative analysis based on cell:stroma ratio, regardless of cytology. The following definitions were used: MLS <25% cell/stroma; TLS $\geq 25\%$ and <50% cell/stroma; RCLS $\geq 50\%$ cell/stroma. The areas assessed had to fill at least one 200X field to be included. All slides in each case were analyzed using this semi-quantitative method, resulting in a composite percentage of MLS, TLS and RCLS in each case. Adverse outcome was defined as local recurrence or distant metastasis. In addition, Ki67 nuclear stain was assessed in MLS, TLS and RCLS areas in each case.

Results: Patients with $\geq 5\%$ RCLS were significantly more likely to develop distant metastasis than those with <5% RCLS ($p = 0.023$). When partitioning patients into MLS (<5% RCLS and <5% TLS), TLS (<5% RCLS and $\geq 5\%$ TLS) and RCLS ($\geq 5\%$ RCLS) groups, patients in the RCLS group were more likely to have distant metastasis than those in either the TLS or MLS groups ($p = 0.039$). Although a trend towards increased metastasis was noted in the TLS group compared to the MLS group, the result was not statistically significant. Mean Ki67 scores in MLS, TLS and RCLS areas were 1.9, 6.6 and 17.5, and these differences were found to be statistically significant ($p = 0.004$, $p = 0.008$, $p = 0.003$).

Conclusions: Similar to prior studies, our semi-quantitative analysis revealed that round cell differentiation portends an adverse outcome, as patients with $\geq 5\%$ RCLS were significantly more likely to develop distant metastasis. Although no statistically significant increased risk for distant metastasis was noted with TLS, a larger group of cases with TLS would help to clarify the prognostic significance of these areas. Finally, Ki67 scores significantly increase from MLS to TLS to RCLS areas and were found to be statistically significant from one another, suggesting that Ki67 scores could be used as a surrogate to quantify MLS, TLS and RCLS areas.

43 Cytogenetic Evaluation of Osteolipoma: A Study of 3 Unique Cases.

KJ Fritchie, KW Rao, JB Renner, RJ Esther. Cleveland Clinic, OH; University of North Carolina Hospitals, Chapel Hill.

Background: Osteolipoma is a rare variant of lipoma consisting of a variable admixture of mature adipose tissue and mature lamellar bone. While typical lipomas are usually not a diagnostic challenge, osteolipomas are rare and may be misclassified by pathologists as benign osseous/cartilaginous lesions or even atypical lipomatous tumors. Translocations involving 12q13-15 are the most common alterations seen in lipomas, and as such, the identification of translocations involving 12q13-15 may aid in the correct diagnosis of osteolipoma.

Design: We examined the clinical and radiologic findings, histologic features and karyotypes of three mature lipomatous tumors with bone formation. These tumors were initially classified as lipoma, atypical lipomatous tumor and juxta-articular chondroma.

Results: Two lesions encased the patellar tendon, while the third abutted the extensor carpi radialis longus and brevis. No connection to bone was noted in any of the lesions. The lesions measured 5.2 cm, 4.0 cm and 3.4 cm. Histologic examination revealed mature lipomatous tumors with varying amounts of chondroid and osseous

elements without cytologic atypia. Cytogenetic analysis reveal a t(3;12)(q27;q13-15) in all three cases, with the following abnormal karyotypes: 46,XX,t(3;12)(q27;q15) [10], 46,XX,t(3;12)(q27;q13) [18] / 46,XX[2], and 46,XY,t(3;12)(q27;q14-15) [15] / 46,XY[4].

Conclusions: Osteolipomas are uncommon benign lipomatous tumors that may present a diagnostic challenge for pathologists unfamiliar with this entity. Cytogenetic analysis utilizing fresh tissue can aid in the diagnosis of these tumors and prevent misclassification.

44 Histologic Spectrum of Myxoid Liposarcoma: Potential Diagnostic Pitfalls on Core Needle Biopsy.

KJ Fritchie, JR Goldblum, RR Tubbs, Y Sun, SD Billings, BP Rubin. Cleveland Clinic, OH.

Background: A wide variety of histologic patterns have been observed in myxoid liposarcoma. The diversity of these patterns can lead to diagnostic difficulty and misclassification, particularly in small biopsy specimens.

Design: We examined the morphologic spectrum of myxoid liposarcoma by cataloguing the patterns identified in the biopsy and resection specimens of 47 primary, recurrent and metastatic tumors in 37 patients.

Results: Patterns identified included: traditional myxoid (94%), traditional round cell (36%), hypercellular myxoid (so-called "transitional") (83%), pseudoacinar (51%), lipoblast-rich (28%), island (26%), stromal hyalinization (17%), lipomatous (17%), cord-like (11%), aggregate (6%), chondroid metaplasia (4%) and HPC-like (2%). Tumors with significant amounts of the lipomatous pattern had large areas that resembled mature adipose tissue potentially leading to misclassification as lipoma or atypical lipomatous tumor. Foci of chondroid metaplasia led to consideration of entities including mixed tumor and cartilaginous neoplasms, while tumors with the cord-like pattern raised consideration for extraskeletal myxoid chondrosarcoma and carcinoma. We also identified two patterns not previously described: aggregate and HPC-like patterns. The aggregate pattern was characterized by grape-like clumps of neoplastic cells in a myxoid background, while the HPC-like pattern consisted of staghorn vessels surrounded by closely packed round cells. The diagnosis of myxoid liposarcoma was confirmed by fluorescence in situ hybridization studies for *CHOP (DDIT3)* translocation in all cases in which paraffin-embedded tissue was available for analysis.

Conclusions: The morphologic spectrum of myxoid liposarcoma is vast and spans beyond the well recognized traditional myxoid and round cell histologies. Awareness of the variety of histologic patterns in myxoid liposarcoma is critical to avoid misdiagnosis, especially in small biopsy specimens.

45 Ossifying Fibromyxoid Tumor of Soft Parts (OFMT): A Clinicopathologic, Proteomic and Genomic Study.

RP Graham, SM Dry, X Li, SW Binder, A Dogan, AL Folpe. Mayo Clinic, Rochester, MN; UCLA, Los Angeles, CA.

Background: OFMT, rare neoplasms of uncertain differentiation, are usually histologically and clinically benign. However, some OFMT are histologically malignant and aggressive, and the behavior of all OFMT may be unpredictable. We studied the clinicopathological features of a large series of OFMT and performed paraffin section proteomic and DNA microarray studies, to more fully elucidate their behavior and differentiation.

Design: 38 OFMT were retrieved and classified as "typical" (OFMT-T), "atypical" (OFMT-AT) and "malignant" (OFMT-M) using published criteria. Follow-up (F/U) was obtained. For proteomics, formalin-fixed, paraffin-embedded (FFPE) blocks from 5 OFMT-T were microdissected, trypsin digested, and analyzed by mass spectrometry. Data was correlated to fragmentation patterns of peptide sequences (Swissprot database). For genomics, total RNA was isolated from FFPE blocks of 7 OFMT-T and hybridized to the Affymetrix Human U133plus 2.0 Array. AGCC imaging software and Partek Genomics Suite Version 6.4 were used.

Results: OFMT-T (N=19) occurred in 10M/9F (median 51 yrs) in various soft tissue (ST) locations (median size 3 cm, range 1.1-11 cm). OFMT-AT (N=8) occurred in 5M/3F (median 43 yrs) in diverse ST locations (median size 3.2 cm, range 1.5-8.5 cm). OFMT-M (N=11) occurred in 10M/9F (median 51 yrs) in varied ST locations (median size 3 cm, range 1-11 cm). Clinical f/u >12 mos was available for 10/19 OFMT-T (median 51 mos, range 12-149 mos), 2/8 OFMT-AT (66 and 131 mos) and 7/11 OFMT-M (median 22 mos, range 12-100 mos). All OFMT-T and OFMT-AT with F/U were alive without disease. For OFMT-M with F/U, 4 were without disease, 1 was alive with local recurrence (LR), and 2 were dead of disease, with LR and metastases. Proteomic results included abundant collagens 1A2, 1A1 and 6A3 and S-100 protein; collagen II (cartilage) was absent. Genomic results showed OFMT to be distinct from nerve sheath tumors, with high level expression of neuron-associated genes, including *HuC* and *SLC1A3*, and low levels of schwann cell and/or cartilage associated genes, including *PMP22*.

Conclusions: The results of this, the first proteomic and genomic study of OFMT, suggest that these rare, enigmatic tumors differentiate along neuronal, rather than schwannian or cartilaginous lines, as has been previously suggested. On-going immunohistochemical studies should help to validate these results in larger numbers of cases. Our study confirms the validity of the current classification of OFMT, with clinically malignant behavior being seen only in OFMT-M, but not in OFMT-T or OFMT-AT.

46 Dedifferentiated Chondrosarcoma with Low Grade Dedifferentiated Component – A Single Institutional Study.

MR Hameed, J Healey, C Morris, P Boland, MJ Klein. Memorial Sloan-Kettering Cancer Center, New York, NY; Memorial Sloan-Kettering Cancer Center, New York, NY; Hospital for Special Surgery, New York, NY.

Background: Dedifferentiated chondrosarcoma is a highly malignant sarcoma composed of two divergent histologies, a low-grade cartilaginous component and a high-grade noncartilaginous sarcomatous component. Typically, the low-grade component is a grade 1 chondrosarcoma and the high-grade component is an anaplastic sarcoma such as an osteosarcoma or undifferentiated pleomorphic sarcoma. This tumor usually affects patients over 50 years and most commonly occurs in long bones; it is highly lethal with less than 10% survival after 1 year. Generally the dedifferentiated component is resistant to chemotherapy and radiation therapy. Dedifferentiation to a low grade mesenchymal component such as low grade osteosarcoma or fibrosarcoma is extremely rare.

Design: The objective of this study was a retrospective review of dedifferentiated chondrosarcomas from 1984-2009 from Pathology Department of MSKCC files to identify cases with low-grade dedifferentiation and to correlate pathological findings with outcome. Materials and Methods: Following IRB approval and SNOMED search, thirty four cases with available slides, resected at MSKCC were identified.

Results: There were 19 males and 15 females. Patient age group ranged from 21 to 96 years. Location of the tumor is as follows: femur (19), pelvis (9), humerus (3), scapula (2) and chest wall (1). Tumor size ranged from 2.3 cm to 27 cm. Tumor was confined within bone in 3 out of 34 cases. In a majority of cases (76%), the chondrosarcomatous component was grade II or I-II. The dedifferentiated component consisted of either a high grade spindle cell sarcoma or a pleomorphic undifferentiated sarcoma in 24 out of 34 cases (70%). The remainder were pleomorphic sarcoma and osteosarcoma (5), osteosarcoma (4) and fibrosarcoma (1). In addition, 7 cases (20%) had areas of low grade spindle cell dedifferentiation comprising about <5% to 80% of the dedifferentiated component. Follow up was available for 26 patients (1.5-46 months). Sixteen patients were dead and ten are alive, two with metastatic disease. In this group, three of four patients with areas of low grade dedifferentiation are alive (11-33 months).

Conclusions: Low grade dedifferentiation can be seen in dedifferentiated chondrosarcoma. Awareness of this phenomenon is important especially in biopsy specimens. Rarely this histology can be predominant.

47 DOG-1 Expression in Non-Gastrointestinal Stromal Tumor (GIST) Neoplasms.

J Hemminger, J Mayerson, W Kraybill, T Scharschmidt, H Iwenofu. The Ohio State University Medical Center, Columbus.

Background: Accurate and practical diagnosis of gastrointestinal stromal tumors (GISTs) is of great importance given the therapeutic benefit of KIT and PDGFRA tyrosine kinase inhibitors. Recently, a transmembrane calcium-regulated chloride channel protein, discovered on GIST-1 (DOG1), has been shown to be sensitive and specific for GISTs. Thus far, studies of the commercially available DOG1 antibody clone K9 (Novocastra) have primarily focused on spindle cell neoplasms in the differential diagnosis of GISTs. Here, we further characterize DOG1 by studying immunohistochemical (IHC) staining patterns in a range of mesenchymal and epithelial tumors.

Design: A formalin-fixed paraffin-embedded block was obtained for each of the following tumors (n=155): GISTs, epithelioid (n=10) and spindle (n=10) types; melanoma, epithelioid (n=10) and spindle/desmoplastic (n=9) types; schwannoma (n=10); neurofibroma (n=10); leiomyosarcoma (n=10); low grade fibromyxoid sarcoma (n=5); angiosarcoma, epithelioid (n=3), spindle (n=5), and mixed (n=2) types; epithelioid sarcoma (n=5); clear cell sarcoma (n=3); synovial sarcoma (n=10); malignant peripheral nerve sheath tumor, epithelioid (n=1) and spindle (n=10) types; alveolar soft part sarcoma (n=3); chordoma (n=5); pleomorphic undifferentiated sarcoma (n=5); perineurioma (n=4); adenocarcinoma, lung (n=5), colon (n=5), endometrial (n=5); renal cell carcinoma, clear cell (n=5) and chromophobe (n=5) types. Utilizing standard IHC staining protocols, full sections were stained with DOG1 antibody clone K9. Staining was assessed for intensity (1-3+), percentage of tumor positivity, and location.

Results: Of the 20 GISTs, 95% (19/20) expressed DOG1. Over half (11/20) were diffusely positive (>95%) with moderate to strong intensity (2-3+). Evaluation of epithelial neoplasms, revealed focal staining of colorectal (2/5) and endometrial (2/5) adenocarcinomas of 2+ intensity with the percentage of tumor cells ranging from <5 to 40%. DOG1 stained the luminal aspects, and, in one colorectal tumor, staining was cytoplasmic and membranous. One case of schwannoma showed focal (5%) staining of 2+ intensity. The remainder of the neoplasms did not express DOG1.

Conclusions: Our study supports that DOG1 is a highly sensitive and specific marker for GISTs. Herein, we also describe DOG1 positivity in colorectal and endometrial adenocarcinomas with prominent luminal pattern as well as an instance of focal expression in a schwannoma. Given the novelty of DOG1, the staining patterns of these non-GIST neoplasms require further characterization in a large cohort study.

48 Expression of Markers of Chondrocyte Development in Chondroblastoma and Chondromyxofibroma.

DH Hwang, AG Montag. University of Chicago, IL.

Background: Chondrocytes arise from mesenchymal precursors and proceed through distinct stages of development. Chondroblastoma (CB) and chondromyxofibroma (CMF) are benign tumors of bone that have been shown to express some markers that are also expressed during normal chondrocyte development, but the stage of differentiation has not been well characterized.

Design: A tissue microarray was created using 57 chondroblastoma specimens from 34 patients and 11 chondromyxofibroma specimens from 8 patients. The microarray was

stained for the following markers grouped by stage of chondrocyte development: Early (fibronectin, N-cadherin, SOX9, collagen I), Mid (SOX9, IGF-1R, aggrecan, PTHrP, STAT1), and Late (beta-catenin, VEGF, collagen I). SOX9 is expressed in both early and mid stages and collagen I is expressed in both early and late stages. These were evaluated using the following scale: 0 (no staining), 1 (<5% staining), 2 (5-50% staining), 3 (>50% staining). Scores of 2 or 3 were considered positive for that marker.

Results: Greater than 50% of specimens of both CBs and CMFs show expression of fibronectin, SOX9, aggrecan, and PTHrP. 86% of CBs show expression of VEGF versus 50% of CMFs, whereas 100% of CMFs express collagen I versus 34.1% of CBs. Both CMFs and CBs show low (less than 50% of specimens) expression of N-cadherin, IGF-1R, STAT1, and beta-catenin.

Percent of Specimens with Positive Expression (Score 2 or 3)

Marker	CB	CMF	Source
Fibronectin	78	60 (p=0.24)	Sigma
N-cadherin	0	10 (p=0.02)	Dako
SOX9	78	56 (p=0.17)	R&D System
IGF-1R	25	30 (p=0.74)	Cell Signaling
Aggrecan	80	90 (p=0.44)	Abcam
PTHrP	98	56 (p<0.01)	Novus
STAT1	18	22 (p=0.80)	Cell Signaling
Beta-catenin	22	20 (p=0.91)	Zymed
VEGF	86	50 (p=0.01)	Santa Cruz
Collagen I	34	100 (p<0.01)	Abcam

Conclusions: Both chondroblastomas and chondromyxofibromas show marker positivity for all three development stages, but with increased positivity for the mid stage markers. Chondroblastoma shows increased positivity for VEGF, which is a late stage marker.

49 p63 Immunohistochemical Staining Is Limited in Soft Tissue Tumors.

VY Jo, CDM Fletcher. Brigham and Women's Hospital, Boston, MA.

Background: p63, a p53 homolog required for epithelial development, is usually expressed in various normal epithelial tissues and epithelial malignancies. Immunohistochemical detection of p63 is used to identify myoepithelial/basal cells, confirm squamous differentiation, and in the differential diagnosis of spindle cell lesions. However, the distribution of p63 expression in mesenchymal lesions has not been characterized. We examined p63 expression in a large series of soft tissue tumors.

Design: Cases were retrieved from the authors' files. All diagnoses were based on standard and widely accepted criteria. p63 immunohistochemistry was performed using a mouse monoclonal antibody (Neomarkers, clone 4A4, Fremont, CA) at a 1:600 dilution with antigen retrieval by citrate buffer and microwave. Appropriate positive and negative controls were used. Nuclear staining was recorded as positive (diffuse, focal) or negative.

Results: 610 soft tissue tumors (whole sections) were examined for p63 expression by immunohistochemical staining. Nuclear reactivity for p63 was found in the following entities: myoepithelial carcinoma (8/20), cellular neurothekeoma (12/20), perineurioma (4/20), EWS/PNET (7/20), and diffuse-type giant cell tumor (5/20). Tumors showing infrequent, weak, or focal positivity were LGFMS (1/10), MPNST (1/20), extraskeletal myxoid chondrosarcoma (1/10), myxofibrosarcoma (1/20), epithelioid sarcoma (2/20), synovial sarcoma (1/20; glands only), embryonal RMS (1/10), DSRCT (1/10), AFX (1/20), and spindle cell melanoma (1/20). No expression of p63 was seen in all other tumor types evaluated: angiosarcoma, Kaposi sarcoma, atypical lipomatous tumor/well-differentiated liposarcoma, dedifferentiated liposarcoma, myxoid liposarcoma, spindle cell lipoma, cellular fibrous histiocytoma, DFSP, desmoid fibromatosis, nodular fasciitis, SFT, leiomyosarcoma, alveolar RMS, IMT, neurofibroma, schwannoma, so-called angiomatoid MFH, GIST, PECOM, ossifying fibromyxoid tumor, alveolar soft part sarcoma, clear cell sarcoma, follicular dendritic cell sarcoma.

Conclusions: p63 immunoreactivity is limited in soft tissue tumors, with the large majority of entities showing negative or at most focal staining. Similar to prior reports, 40% of myoepithelial carcinomas were p63-positive. Interestingly, at least weak p63 expression was observed in over 50% of cellular neurothekeomas and in a subset of cases of perineurioma, EWS/PNET, and diffuse-type giant cell tumor, the significance of which is uncertain. Absent p63 expression is typical for most soft tissue tumors, including most that would be in the differential diagnosis of spindle cell squamous carcinoma.

50 Epithelioid Rhabdomyosarcoma: A Morphologically Distinct Variant.

VY Jo, CDM Fletcher. Brigham and Women's Hospital, Boston, MA.

Background: Rhabdomyosarcoma (RMS) mainly affects children and young adults and is currently classified into embryonal, alveolar, and pleomorphic subtypes. RMS is rare in older adults and in these patients the pleomorphic variant is most common. All RMS subtypes show immunohistochemical evidence of rhabdomyoblastic differentiation. We have identified a seemingly distinct RMS variant that demonstrates epithelioid features, reminiscent of poorly differentiated carcinoma or melanoma, and occurring mostly in older adults.

Design: Fifteen cases of epithelioid RMS identified between 2001 and 2009 were retrieved from consultation files. H&E and immunohistochemical stains were examined. Clinical and follow-up information was obtained from referring pathologists.

Results: Affected patients were 10 men and 4 women (1 unknown sex), with median age of 70 years (range 14-78). Ten tumors were intramuscular and 2 were subcutaneous. Anatomic sites were upper extremity (4), lower extremity (2), head and neck (3), thoracoabdominal wall (2), back (1). Materials for 3 patients were nodal metastases (neck, mediastinum). Lesions ranged in size from 3 to 8.5 cm, having nodular fleshy cut surfaces, necrosis, and infiltrative edges. All tumors demonstrated high grade epithelioid

features, with abundant amphophilic-to-eosinophilic cytoplasm, large vesicular nuclei and frequently prominent nucleoli. Only mild or very focal pleomorphism was seen. Three tumors had focal rhabdoid inclusions. Tumor cells showed sheet-like growth with prominent necrosis, and 1 case showed prominent nesting. All tumors exhibited infiltrative growth into adjacent skeletal muscle and fat. Mitotic counts ranged from 4 to 85 per 10 HPF (median 23), with frequent atypical forms. All tumors showed diffuse desmin immunoreactivity; myf4 staining was diffuse to multifocal in 13 cases and more focal in 2 cases. Immunohistochemical stains for keratins and S100 were negative in all cases. Most patients underwent surgical resection with chemotherapy and/or radiation. Follow-up information is available for 10 cases so far. One patient had multiple local recurrences, 2 developed satellite nodules near the primary tumor, 6 developed local lymph node metastases, and 5 patients developed distant metastases (lung, bone, liver). Six patients have died of disease (5 within 1 year, 1 within 5 years).

Conclusions: Epithelioid RMS appears to be a morphologically distinct variant of RMS, affecting primarily older patients. These tumors show close mimicry of carcinoma or melanoma, but all exhibit skeletal muscle differentiation by immunohistochemistry. The clinical course as determined thus far is aggressive.

51 Occasional Staining for P63 in Malignant Epithelioid Vascular Tumors.

ME Kallen, FG Nunes, AL Gonzalez, JM Cates, ME Sanders. Vanderbilt Medical School, Nashville, TN.

Background: The tumor protein p63 is involved in a complicated network of molecular interactions controlling cell differentiation and proliferation, and appears to be a useful marker to differentiate between spindle cell carcinoma and sarcoma. Although preliminary studies have demonstrated excellent specificity for epithelial tumors, a limited number of sarcomas have been studied thus far. Recently, we observed serendipitous staining for p63 in an angiosarcoma of the breast. Since none of the previously reported angiosarcomas or epithelioid hemangioendotheliomas examined for p63 expression was positive, we reasoned that further investigation of p63 immunoreactivity in vascular tumors was warranted.

Design: Representative cases of conventional angiosarcoma, epithelioid angiosarcoma, epithelioid hemangioendothelioma and Kaposi sarcoma were identified retrospectively. Immunohistochemical stains for p63 were performed on one selected block from each case. Immunoreactivity was scored as either cytoplasmic or nuclear and the percentage and intensity of positive cells was recorded.

Results: Only 3 of the 35 malignant vascular tumors studied were positive for nuclear p63 (8.6%). However, all three p63-positive cases demonstrated epithelioid-type morphology, with copious eosinophilic cytoplasm. In epithelioid hemangioendothelioma, nuclear staining of moderate intensity (less intense than internal control squamous epithelia) was observed in approximately 60% of neoplastic cells in one case and between 5-10% of tumor cells in another. The one p63-positive epithelioid angiosarcoma showed strong nuclear staining in approximately 75% of cells. In two other cases each of epithelioid angiosarcoma and epithelioid hemangioendothelioma, diffuse and intense cytoplasmic staining for p63 was noted.

Conclusions: Expression of p63 in tumors of vascular differentiation is very unusual, but is seen in occasional cases with an epithelioid morphology (3 of 10 such cases). Since both epithelioid angiosarcoma and epithelioid hemangioendothelioma may also co-express cytokeratins, the finding of nuclear p63 represents another potential pitfall in the differential diagnosis between poorly-differentiated carcinomas and epithelioid vascular neoplasms.

Nuclear p63 staining in vascular tumors.

Diagnosis	Total cases	p63-positive
Angiosarcoma	5	0
Epithelioid angiosarcoma	5	1
Epithelioid hemangioendothelioma	5	2
Kaposi's sarcoma	20	0

52 A Subset of Osteosarcomas Is Positive for Nuclear Expression of P63.

ME Kallen, ME Sanders, AL Gonzalez, JM Cates. Vanderbilt University Medical School, Nashville, TN.

Background: The p63 protein is involved in a complicated network of molecular interactions controlling cell growth and proliferation. Recently, p63 expression has been reported in the mononuclear stromal cells of giant cell tumors of bone, which are now thought likely to be osteoblast-precursor cells. Only a limited number of osteoblastic tumors have been studied for p63 expression by immunohistochemistry thus far. Therefore, we investigated whether p63 may serve as a marker for osteoblastic differentiation in a large series of osteosarcomas.

Design: 172 samples of osteosarcoma, consisting of 105 osteoblastic, 23 fibroblastic, 19 chondroblastic, 3 telangiectatic, 4 small cell, 7 parosteal, 4 low-grade intramedullary, 5 high-grade surface, and 2 periosteal subtypes from 112 patients represented on a tissue microarray were stained for the p63 tumor protein by immunohistochemistry. Associations between selected clinicopathologic parameters and nuclear or cytoplasmic p63 expression were subsequently assessed by exploratory statistical analyses. Kaplan-Meier survival curves were compared using the log-rank test.

Results: Overall, nuclear p63 was detected in only 17 of 172 (9.9%) of samples. Cytoplasmic staining was noted in an additional 41 (23.8%) of cases. There were no statistically significant associations between nuclear or cytoplasmic p63-positive cases and chemotherapy status (naïve vs. treated), specimen type (biopsy, primary resection, local recurrence or metastasis), anatomic location (appendicular vs. axial/pelvic) or histologic subtype. There were no correlations with patient age, response to neoadjuvant chemotherapy (percent coagulative tumor necrosis), or proliferative index (% Ki67-positive cells). Although none of the low-grade osteosarcomas studied were positive

for nuclear p63, this association did not reach statistical significance. No differences in overall, metastasis-free or disease-free survival in p63-positive cases were detected.

Conclusions: Only a small proportion (approximately 10%) of osteosarcomas demonstrates nuclear staining for p63. This subset did not show statistically significant associations with selected clinicopathologic parameters. These findings show that p63 is not useful as a marker of osteoblastic differentiation in malignant bone tumors. However, pathologists should be aware that nuclear p63 positivity is not necessarily indicative of epithelial or myoepithelial differentiation.

53 SOX10 and S100 in the Diagnosis of Soft Tissue Neoplasms.

JR Karamchandani, T Nielsen, M Van de Rijn, RB West. Stanford University Medical Center, CA; University of British Columbia, Vancouver, Canada.

Background: SOX10 is involved in neural crest differentiation, and consistently expressed in melanocytic and schwann cells (Am J Surg Pathol 2008;32:1291-1298). S100 is commonly employed by pathologists to determine if a tumor has neural or melanocytic differentiation, though S100 also stains numerous benign and malignant soft tissue tumors and tissues that are not thought to arise from neural crest tissue (cartilage, dendritic cells, etc.). We compared SOX10 and S100 protein expression in soft tissue tumors to determine which antibody is more specific in identifying soft tissue tumors of neural crest origin.

Design: We compared the results of SOX10 and S100 protein expression in 989 specimens, which included 71 types of neoplasm (predominantly soft tissue), and 33 normal tissues. The majority of the samples were analyzed on tissue microarrays. We also evaluated 20 full cross sections.

Results: Both SOX10 and S100 reliably stained schwannomas (50 cases), neurofibromas (55 cases), and staining was similar in cases of malignant peripheral nerve sheath tumors (78 cases). In 7 of 9 cases of desmoplastic melanoma, SOX10 showed a greater intensity of staining than S100. SOX10 also showed greater intensity of staining in 4/7 cases of clear cell sarcoma, 3 of which were S100 negative. We identified 5 non-neural, non-melanocytic sarcoma types in which a subset of cases showed strong S100 expression but where no SOX10 expression was seen: synovial sarcoma (12/79), Ewings sarcoma (3/14), rhabdomyosarcoma (4/17), chondrosarcoma (3/4), and extraskeletal myxoid chondrosarcoma (5/11). We also studied 550 cases representing 38 benign and malignant soft tissue neoplasms, including adipocytic, smooth muscle, skeletal muscle, vascular, and fibrohistiocytic tumors, as well as several reactive pathologies and tumors of uncertain differentiation. None of these samples showed SOX10 positivity. 20 of these cases showed spurious S100 staining.

Conclusions: SOX10 is a reliable marker of neural crest differentiation, and is consistently expressed in schwannian and melanocytic tumors. In our series, SOX10 proved superior to S100 in the detection of desmoplastic melanoma, and clear cell sarcoma. We did not see SOX10 expression in cases of synovial sarcoma, Ewings sarcoma, rhabdomyosarcoma, chondrosarcoma, or extra-skeletal myxoid chondrosarcoma, all of which occasionally demonstrated strong S100 positivity. Compared to S100, SOX10 shows increased specificity for tumors of neural crest origin, and should be used in the place of S100 in soft tissue tumor diagnosis.

54 Intraarticular Epithelioid Sarcoma (ES): Report of Two Cases, with Immunohistochemical and Molecular Cytogenetic INI-1 Study.

K Kosemehmetoglu, G Kaygusuz, A Bahrami, SC Raimondi, AL Folpe. Ankara Atatürk Education and Research Hospital, Turkey; Ankara University Ibn-i Sina Hospital, Turkey; St. Jude Children's Research Hospital, Memphis, TN; Mayo Clinic, Rochester, MN.

Background: ES, a rare sarcoma with epithelial differentiation, most often occurs in the distal extremities but may occur in essentially any location. With the recent recognition that the loss of expression of the tumor-suppressor gene *INI-1* may be associated with ES, it has become clear that ES may occur in previously unsuspected locations, such as bone. Here we report 2 cases of ES occurring within the knee.

Design: Two intra-articular cases coded as ES were retrieved from our archives. Both were immunopositive for cytokeratins (AE1/AE3 and OSCAR), CD34, vimentin, and epithelial membrane antigen, and both showed complete loss of expression of INI-1. Six cases coded as malignant pigmented villonodular synovitis (M-PVNS) were also retrieved and immunostained for the same markers using commercial antibodies and the Dako EnVision system. FISH was performed on formalin-fixed, paraffin-embedded sections by using a laboratory-developed dual-color probe containing INI1 [CTD-2511E13 + CTD-2034E7] (22q11.2) (OR) and PAXX2 [RPCI3-402G11] (22q13.33) (GR) probe as control.

Results: Both cases of SE occurred in a clearly intra-articular location in the knee. Case 1 was that of a 60-year-old woman. Follow-up information available for this patient showed bilateral subpleural nodules that were radiographically consistent with metastases. Case 2 was that of a 19-year-old man with a long-standing history of pain and limited joint function. Morphologically, both tumors showed features of proximal-type ES with prominent rhabdoid morphology. Although immunohistochemistry of both tumors showed a complete loss of INI-1 protein, FISH analyses were negative for *INI-1* gene deletion in both cases. The 6 cases of M-PVNS were negative for nearly all of the tested markers; INI-1 expression was retained.

Conclusions: Here we have reported, to the best of our knowledge, the first cases of intra-articular ES. The morphological and immunohistochemical features of this tumor are identical to those of ES in conventional locations, including loss of *INI-1* expression. The loss of INI-1 protein expression in the absence of *INI-1* gene deletion might distinguish proximal-type ES from malignant extrarenal rhabdoid tumor. Although we were not able to identify any additional cases of intra-articular ES within the 6 cases previously diagnosed as M-PVNS, intra-articular ES should be rigorously excluded before making the latter diagnosis.

55 Frequent Expression of Fibroblast Growth Factor-23 (FGF-23) mRNA in Aneurysmal Bone Cyst (ABC).

S Krishnamurthy, CY Inwards, AM Oliveira, AL Folpe. Mayo Clinic, Rochester, MN.

Background: The great majority of cases of tumor-induced osteomalacia (TIO) are caused by a morphologically distinctive soft tissue and bone tumor, known as phosphaturic mesenchymal tumor, mixed connective tissue type (PMT). In almost all instances PMT produce TIO through secretion of FGF-23, a phosphaturic hormone. We have previously shown detection of *FGF-23* by RT-PCR in formalin-fixed, paraffin-embedded (FFPE) tissues to be a valuable adjunct to this sometimes difficult diagnosis. However, TIO caused by other mesenchymal tumors (e.g., polyostotic fibrous dysplasia) is well documented, suggesting that FGF-23 expression may not be unique to PMT. Prompted by our earlier findings of FGF-23 expression in 1 ABC and 1 chondromyxoid fibroma (CMF) of flat bone type, we examined a larger series of ABC and CMF for *FGF-23* expression.

Design: FFPE blocks from 13 cases with typical morphologic and radiographic features of ABC (8) and CMF (5) were retrieved from our archives. The clinical records of all patients were reviewed. RT-PCR for *FGF-23* was performed using our previously published methods.

Results: The 13 tumors studied occurred in 8 men and 5 women ranging in age from 8 to 75 years (mean, 27 yrs). All of the tumors involved bone, including 2 in the skull, 4 in the spine, 2 in the upper extremity (1 each in metacarpal and ulna), 3 in the lower extremity (2 in tibia and 1 in acetabulum), and 1 each in the rib and clavicle. None of the patients had evidence of TIO in the clinical records. One ABC and 2 CMF did not contain amplifiable mRNA and were excluded. RT-PCR for *FGF-23* was positive in 4/7 (57%) of the ABCs. None of the CMF were positive.

Conclusions: The results of the present study confirm and amplify our previous finding of *FGF-23* expression in a subset of ABCs, all with typical clinical, radiographic and morphologic features, and without any features suggestive of PMT. This finding is intriguing, inasmuch as calcified matrix resembling that seen in many PMT is often identified in ABC. It is unclear whether *FGF-23* expression is related to the distinctive morphologic features of ABC, or is simply an epiphenomenon. Most importantly, these findings emphasize that the diagnosis of PMT, as with any diagnosis, must rest on an integration of all clinical, radiographic and laboratory findings, and must not rely on *FGF-23* studies alone.

56 MDM2-p53 Pathway Status in Clinical Samples of Well-Differentiated and Dedifferentiated Liposarcoma.

A Kumagai, T Motoi, A Yoshida, T Imamura, T Fukusato. Teikyo University School of Medicine, Tokyo, Japan; University of Tokyo, Japan; Teikyo University Hospital, Tokyo, Japan.

Background: Well-differentiated liposarcoma (WLPS) and dedifferentiated liposarcoma (DLPS) are genetically characterized by *MDM2* gene amplification. Although overexpressed MDM2 is generally believed to suppress p53 function, the status of MDM2-p53 pathway in clinical tumor samples has not been investigated. In this study, tumor cell type-specific status of MDM2-p53 pathway was examined by immunohistochemistry, chromogenic in situ hybridization (CISH), and by measuring microRNAs (miR)-34a, a known target of p53.

Design: Formalin-fixed paraffin-embedded tissue samples of 6 WLPSs and 5 DLPSs containing pairs of dedifferentiated (DD) and well differentiated components (DW) were studied. Tumor cells were morphologically subclassified into 3 groups; adipocyte-like cells and non-adipocyte-like cells in DW and WLPS, and dedifferentiated cells in DD. CISH was performed using dual-color-labeled probes for *MDM2* and *CEN12*. The number of amplified signals (*MDM2/CEN12* > 2.0) was counted in 60 nuclei. The number of immunopositive cells was counted in 100 nuclei for MDM2 and p53. The expression of miR-34a was measured by quantitative real-time RT-PCR. Four normal adipose tissues and 5 lipomas were used as controls.

Results: In DLPSs, *MDM2* gene amplification, MDM2 and p53 immunopositivity occurred in 33.8%, 8.0%, and 1.7% of adipocyte-like cells; in 54.2%, 30.3%, and 8.6% of non-adipocyte-like cells; and in 75.2%, 41.0%, and 22.5% of dedifferentiated cells. In WLPSs, they occurred in 45.5%, 11.5%, and 5.1% of adipocyte-like cells; and 65.9%, 29.2%, and 8.4% of non-adipocyte-like cells. Adipocyte-like cells showed significantly less positivity for *MDM2* amplification and MDM2 expression compared with the other 2 cell types. Dedifferentiated cells were significantly more positive for p53 than the other 2 cell types. miR-34a expression was significantly higher in liposarcomas than controls ($p < 0.05$), whereas it was comparable among different components of liposarcoma.

Conclusions: The status of *MDM2* amplification may reflect the intratumoral heterogeneity. *MDM2* amplification and overexpression inversely correlated with adipocytic differentiation. Uncoordinated immunopositivity of MDM2 and p53 indicates dysregulated MDM2-p53 pathway. Constant overexpression of miR-34a regardless of liposarcoma subtypes further suggests that p53 activity is up-regulated rather than suppressed. In conclusion, p53 may not be controlled by MDM2 in liposarcoma contrary to popular belief.

57 Primary Myoepithelioma of Bone.

PJ Kurzawa, PG Nielsen, S Kattapuram, FJ Hornicek, AE Rosenberg. Great Poland Cancer Centre, Poznan, Wielkopolska, Poland; Massachusetts General Hospital, Boston.

Background: Myoepithelial tumors are diverse in their morphology and biology. They are composed of neoplastic cells that may be purely myoepithelial in phenotype (myoepithelioma) and in some cases these tumors may also contain a second population of cells that are epithelial in differentiation. Recently, this tumor has been shown to harbor a rearrangement of the *EWSR1* gene on chromosome 22 in 45% of cases.

Myoepithelioma has been described to arise in salivary glands, skin, upper airway, lung, gastrointestinal tract, breast, soft tissue, and rarely in bone. To increase our understanding of intra-osseous myoepithelioma we reviewed our experience with 8 cases.

Design: The study cohort was identified from the authors consult files and from the surgical pathology files of MGH. The clinicopathologic characteristics of the tumors including their histologic and immunohistochemical features, and status of translocation involving the *EWSR1* gene were analyzed.

Results: The patients included 5 females and 3 males who ranged in age from 16-49 (mean of 33.5) years. The tumor locations included: 3 in the ilium, 2 in the tibia, and 1 each in the maxilla, sacrum, and L1. Radiographically 6 of the lesions were limited to the bone and were lytic or mixed sclerotic and lytic in appearance. Two tumors breached the cortex and extended into the soft tissues and grew with pushing margins. Histologically the tumors were composed predominantly of spindle cells with variable numbers of epithelioid cells some of which had clear or eosinophilic cytoplasm. The stroma was hyalinized, collagenous or myxoid. Immunohistochemically, all tumors were positive for S-100 and 7 were positive for EMA (1 negative case had a *EWSR1* gene rearrangement). None of the tumors were positive for keratin cocktail. FISH for *EWSR1* rearrangement was performed in 7 tumors; 5 tumors (71%) were positive and 2 tumors (29%) were negative. Treatment in 5 patients consisted of curettage, 1 is scheduled to be resected in the near future and the data of two patients is not currently available. Follow-up available on 3 patients ranges from 4-35 months (mean 18 months) and all have remained free of disease with no local or disseminated recurrence.

Conclusions: Primary myoepithelioma is a rare primary bone tumor and can be confused with a variety of different neoplasms. Immunohistochemically, they usually express S100 and EMA and have a gene rearrangement involving *EWSR1*. In our series the tumors had benign histological features, and although follow-up is limited, they have not behaved in an aggressive fashion.

58 Malignant Fat-Forming Solitary Fibrous Tumor: Clinicopathologic Analysis of 14 Cases.

J-C Lee, CDM Fletcher. National Taiwan University Hospital, Taipei, Taiwan & Brigham and Women's Hospital, Harvard Medical School, Boston, MA.

Background: Fat-forming solitary fibrous tumor (FF-SFT) is a rare variant of solitary fibrous tumor (SFT) containing variable amounts of usually mature fat. Generally deemed benign, FF-SFTs were very rarely reported to have malignant histologic features, at least one case of which recurred and proved fatal. Here we report 14 histologically malignant FF-SFTs to better characterize this subset.

Design: Of 81 FF-SFTs in our consultation files, 14 exhibited malignant features (mitoses $\geq 4/10$ HPF, hypercellularity, atypia, necrosis, and/or infiltrative margins, according to WHO criteria for malignant SFT) and were retrieved for analysis. The histology and immunostains were reviewed, and the clinical parameters and follow-up data were obtained from referring physicians.

Results: Seven patients were female and 7 male, with ages ranging from 20 to 93 years (median 57 years.) Most presented with a slowly enlarging mass, some with recent increase in growth or local discomfort. Five (36%) were located in lower limbs, 3 (21%) in trunk, 3 (21%) in abdominopelvic locations, 2 (14%) in the head or neck, and 1 (7%) in the upper limb. Grossly, the tumor size ranged from 3.4 to 20 cm (median 8.6 cm), all were well-demarcated, and most were yellow-white to pink / tan and rubbery. Histologically, all exhibited at least focal hypercellularity; 12 tumors had more than 4 mitoses /10HPF (range 2-37, median 7.5); 11 showed at least moderate atypia (focal or diffuse); 9 showed necrosis; 1 had focal infiltrative margin. All had variable amount of mature adipose tissue. Of note, 5 contained multivacuolated lipoblasts and 2 had adipocytes of varying size with atypical stromal cells, resembling atypical lipomatous tumor (ALT), which were not observed in the other 67 FF-SFT in our files. By immunohistochemistry, CD34 was positive in 11 of 14 cases tested, CD99 positive in 8 of 9, and MDM2 and CDK4 were both negative in all 3 tested (including both with ALT-like areas.) Follow-up data thus far (9 cases, median duration 55 months, range 2.5-76) showed no local recurrence and 1 patient with metastasis (lung, spine, and bilateral breasts) who died of disease at 57 months.

Conclusions: FF-SFT exhibiting malignant histologic features shows potential for aggressive behavior comparable to conventional malignant SFT. Presence of lipoblasts and/or ALT-like areas seems to be much more common in the malignant subset and may imply concurrent malignant change of both spindle and adipocytic components.

59 Loss of ASS1 Expression in Myxofibrosarcoma Via Promoter Hypermethylation: Prognostic and Potential Therapeutic Implications.

C-F Li, L-T Chen, Y-H Wang, Y-L Shiu, H-Y Huang. Chi-Mei Hosp., Tainan, Taiwan; Institute of Biomedical Sciences, National Sun Yat-Sen University, Kaohsiung, Taiwan; NCRI, NHRI, Tainan, Taiwan; Chang Gung Memorial Hosp., Kaohsiung, Taiwan.

Background: Argininosuccinate synthase 1 (ASS1), catalyzing the penultimate step of the arginine biosynthetic pathway, is commonly downregulated in human cancers. Taking advantage of this deregulated cellular metabolism, pegylated arginine deiminase (ADI-PEG20) has emerged as a novel target therapy that renders ASS1-deficient cancer cells particularly susceptible to arginine deprivation. We herein address ASS1 expression status and its downregulating mechanism, prognostic value, and therapeutic relevance in myxofibrosarcoma (MFS).

Design: Immunopositivity of ASS1 protein was evaluated on tissue microarrays of primary MFS, yielding 90 cases with assessable results for correlation with clinicopathological variables and patient survival. Methylation status of *ASS1* gene promoter was examined by methylation-specific PCR (MSP). Compared with CCD966SK dermal fibroblasts, three MFS cell lines (OH931, NMFH-1, NMFH-2) were analyzed for protein and mRNA levels of ASS1 by immunoblotting and quantitative RT-PCR assays, respectively. XTT assay was performed to evaluate the susceptibility to ADI-PEG20 treatment in three MFS cell lines vs. CCD966SK fibroblasts.

Results: ASS1 deficiency was identified in 40 cases and significantly associated with increment in FNCLCC grade ($p=0.005$), AJCC stage ($p=0.007$), and mitotic activity ($p=0.030$), with remarkable tumor necrosis ($p=0.046$), and univariately with inferior metastasis-free survival (MeFS, $p=0.0052$) and disease-specific survival (DSS, $p=0.0035$). In multivariate comparisons, ASS1 deficiency independently predicted both MeFS ($p=0.0213$, risk ratio [RR]=4.237) and DSS ($p=0.0230$, RR=10.416), along with higher FNCLCC grades. In the first batch subjected to MSP, hypermethylation of ASS1 promoter was identified in 6 of 10 cases and associated with loss of ASS1 immunoexpression ($p=0.004$). Compared to fibroblasts, the endogenous ASS1 mRNA expression was remarkably downregulated in all 3 MFS cell lines (0-, 0.004-, and 0.055-folds), concordant with the hypermethylation of their ASS1 promoters and deficiency in protein expression. In contrast to no susceptibility seen in CCD966SK fibroblasts, ADI-PEG20 at a low concentration (0.1 $\mu\text{g/ml}$) could remarkably attenuate cell viability of 3 MFS cell lines.

Conclusions: Epigenetic promoter methylation may lead to ASS1 deficiency in a significant subset of MFS, which not only confers tumor aggressiveness but also represents a novel target for arginine deprivation therapy.

60 TPD52 Significance in a Large Series of Ewing's Sarcoma Family of Tumors (ESFT). Support: EuroBoNet (European Network of Excellence). Contract No. 018814.

ALlombart-Bosch, I Machado, S Calabuig-Farinas, JA Lopez-Guerrero, M Alberghini, K Scotlandi, P Picci, J Byrne. Valencia University, Spain; IVO, Valencia, Spain; Institute Ortopedico Rizzoli (IOR), Bologna, Italy; Children's Cancer Research, Sidney, Spain.

Background: Tumor Protein D52 (TPD52) was identified in the 8q21 amplicon, and is involved in cellular transformation, proliferation and metastasis. The aim of the present study is to describe the implication of TPD52 in a large series of Ewing's sarcoma (ESFT).

Design: 324 genetically-confirmed ESFT were included in the study. Out of the 324 tumors analyzed, 272 (84%) corresponded to primary localized tumors, 22 (7%) to disseminated primary tumors, 9 (3%) to recurrences, and 21 (6%) to metastases. For the prognostic analysis, we analyzed a cohort of 217 patients with localized disease. TMA sections were immunostained with TPD52 antibody (Sidney, Australia, dilution 1:250). A correlation with the expression of additional IHC markers (pan-CK, occludin, claudin, ZO-1, e-cadherin, desmoglein, snail, slug, AKT1,2, AKT1,2,3, GSK3 β , p-GSK3 β , PI3kin, and ezrin) studied previously in the same series was performed.

Results: ESFT revealed TPD52 expression in 35.5% of the tumors, this protein being more frequently expressed in atypical (21/49, 41%) compared with PNET (8/31, 24%) and conventional (41/117, 35%). Comparing TPD52 expression between localized (52/161, 31.7%) and disseminated (19/36, 52.8%) cases, we observed a significant direct association between TPD52 expression and disseminated tumors ($p=0.015$). The majority of cases with negative IHC results for desmoglein and occludin failed to express TPD52 ($p=0.031$ and $p=0.0001$, respectively). Additionally, the majority of ESFT with positive IHC result for slug, ZO-19 and ezrin revealed positive TPD52 ($p=0.0001$, and $p=0.007$ and $p=0.032$, respectively). In the Kaplan-Meier analysis, TPD52 immunoexpression does not represent prognostic factor for progression free survival/PFS ($p=0.442$) and disease specific survival/DSS ($p=0.237$) in ESFT.

Conclusions: TPD52 is frequently expressed in ESFT, being higher in disseminated cases than in localized tumors. The correlation of TPD52 expression with a number of epithelial markers, adhesion molecules and EMT markers in ESFT may be related with the expression of an epithelial phenotype. TPD52 IHC expression does not represent an independent prognostic factor for PFS and DSS in localized ESFT.

61 Ezrin Significance in a Large Series of Ewing's Sarcoma Family of Tumors. Support: EuroBoNet (European Network of Excellence). Contract No. 018814.

ALlombart-Bosch, I Machado, S Calabuig-Farinas, JA Lopez-Guerrero, M Alberghini, K Scotlandi, P Picci. Valencia University, Spain; IVO, Valencia, Spain; Institute Ortopedico Rizzoli, Bologna, Italy.

Background: Ezrin (a cytoskeletal protein) has been implicated as a conduit for signals between metastasis-associated cell-surface molecules and signal transduction components. The aim of the present study is to describe the implication of ezrin in a large series of genetically-confirmed ESFT and study the clinicopathological significance.

Design: A total of 324 ESFT genetically-confirmed were included in the study. The clinical data were reviewed and stored in a specific database. Out of the 324 tumors analyzed, 272 (84%) corresponded to primary localized tumors, 22 (7%) to disseminated primary tumors, 9 (3%) to recurrences, and 21 (6%) to metastases. For statistical considerations, disseminated primary tumors, recurrences, and metastases were grouped into the same category (disseminated disease). For the prognostic evaluation, we analyzed a cohort of 217 patients with localized disease. IHC and FISH analysis were performed in TMAs (24). TMA sections were immunostained with ezrin antibody (clone 3C12, dilution 1:250).

Results: ESFT revealed ezrin expression in 61% of the tumors, ezrin was more frequently expressed in PNET (60%) compared with atypical (54%) and conventional (39%) ES ($p=0.026$). Ezrin was more frequently expressed in recurrences (100%), metastasis (78%) and disseminated primary tumors (61%), compared with the primary tumor (40%) ($p<0.0001$). Comparing ezrin expression between localized (40%) and disseminated (71%) cases, we observed a significant direct association between ezrin expression and disseminated cases ($p<0.0001$). In ESFT with strong ezrin expression, apoptotic cells did not express ezrin compared with non-apoptotic cells. In the multivariate analysis, ezrin immunoexpression (positive cases) represents an independent good prognostic factor for progression free survival/PFS ($p=0.007$) and disease specific survival/DSS ($p=0.003$).

Conclusions: Ezrin antibody is frequently expressed in ESFT, and does not offer any diagnostic clues for the differential diagnosis with other small round cell tumors of bone (osteosarcoma, chondrosarcoma, etc). Ezrin expression in disseminated cases is more frequently observed than in localized tumors; however, ezrin IHC expression represent an independent good prognostic factor for PFS and DSS.

62 ERG Transcription Factor as a Marker for Vascular Tumors.

M Miettinen, Z-F Wang, S-H Tan, A Dobi, S Srivastava, I Sesterhenn. Armed Forces Institute of Pathology, Washington, DC; Uniformed Services University of Health Sciences, Rockville, MD.

Background: Background: ERG transcription factor belongs to the ETS-family of transcription factors and is involved in tumor translocations observed in a subset of prostate carcinomas. Recently, ERG expression has been detected in vascular endothelial cells. In this study we examined ERG-expression in selected normal tissues, vascular tumors, and non-vascular tumors as controls.

Design: A mouse monoclonal antibody to ERG (Clone 9F4) developed at the Center for Prostate Disease Research was used, with a Leica automatic immunostainer using Leica's avidin-biotin free polymer-based detection system. Diaminobenzidine was used the chromogen. Selected normal tissues and 250 vascular and non-vascular tumors were examined for ERG-immunoreactivity. Only tissues that demonstrated endothelial cell nuclear ERG-immunoreactivity were scored, and only nuclear immunoreactivity was counted as positive. Approximately 10% of examined tissues lacked any ERG-immunoreactivity suggesting that this epitope may be sensitive to suboptimal fixation.

Results: In normal skin, breast, tonsil, thymus, liver, kidney, adrenal, pancreas, thyroid, stomach, colon, and term placenta, nuclear ERG-immunoreactivity was restricted to vascular endothelial cells. Nuclear ERG-positivity was consistently observed in endothelial component of benign vascular tumors ($n = 6$, at minimum in each category): capillary and cavernous hemangiomas of different types, papillary endothelial hyperplasia, and lymphangioma. In spindle cell hemangioma, the endothelial component was positive and spindle cells negative. In malignant vascular tumors, majority of spindle cells and endothelial cells in Kaposi sarcomas ($n = 11$) and tumor cells in epithelioid hemangioendothelioma ($n = 11$) and angiosarcoma ($n = 17$), were positive. All non-vascular tumors (minimum 10 cases of each): glomus tumor, paraganglioma, nodular fasciitis, synovial sarcoma, leiomyosarcoma, gastrointestinal stromal tumor, myxoid liposarcoma, undifferentiated pleomorphic sarcoma (MFH), and malignant mesothelioma were negative showing endothelial cell immunoreactivity only. One pleomorphic liposarcoma showed exceptional nuclear ERG-positivity.

Conclusions: ERG transcription factor is a promising new endothelial cell marker for benign and malignant vascular tumors. Its specificity and sensitivity should be further explored with a larger panel of vascular and non-vascular tumors.

63 Neoadjuvant Radiation: Effect on Immunohistochemical Marker Expression in Soft Tissue Tumors.

B Mitrovic, R Kirsch, PW-M Chung, PC Ferguson, JS Wunder, BC Dickson. Mount Sinai Hospital, Toronto, ON, Canada; UHN Princess Margaret Hospital, Toronto, ON, Canada.

Background: It is generally assumed that immunohistochemistry is unreliable in the setting of neoadjuvant radiation; however, there is limited published data to support this view. The aim of this preliminary study is to assess the reliability of immunohistochemistry in the context of neoadjuvant radiation by comparing the staining patterns of commonly used markers in soft tissue tumors before and after radiation.

Design: We prospectively identified soft tissue tumors resected after neoadjuvant radiation at our institution. The expression of a broad array of markers, with emphasis on common stains such as AE1/AE3, S100, smooth muscle actin, desmin and CD34, was evaluated and compared between pre- and post-treatment specimens.

Results: A total of 24 neoadjuvant specimens were examined: 1 clear cell sarcoma, 1 epithelioid sarcoma, 1 extraskeletal myxoid chondrosarcoma, 1 fibrosarcoma, 1 leiomyosarcoma, 5 liposarcomas, 2 rhabdomyosarcomas (pleomorphic), 3 sarcomas of unknown histogenesis, 1 solitary fibrous tumor, 4 synovial sarcomas and 4 undifferentiated pleomorphic sarcomas. Immunohistochemistry was available on 17 corresponding pre-treatment biopsies. Only minor discrepancies were identified between pre- and post-treatment specimens. Loss of expression was seen in two cases: a clear cell sarcoma with weak expression of synaptophysin that was lost post-therapy, and a rhabdomyosarcoma with focal Myf-4 expression that was lost post-therapy. Post-therapy gain of expression was seen in three cases: a solitary fibrous tumor gained focal AE1/AE3 expression; a synovial sarcoma gained epithelial membrane antigen expression; and another synovial sarcoma gained focal S100 expression.

Conclusions: Overall, there was generally concordance of immunophenotype comparing pre- and post-radiation specimens. Differences were focal and in some cases likely attributable to sampling issues. The loss of Myf-4 in a rhabdomyosarcoma was unexpected and it is unclear whether this reflects altered transcriptional activity due to radiation. Focal keratin expression occasionally occurs in solitary fibrous tumors and it is possible this was exacerbated by radiation. Neoadjuvant radiotherapy appears to minimally affect the immunophenotype of soft tissue tumors, suggesting that immunohistochemistry may retain diagnostic value in the post-neoadjuvant setting. Confirmation of these preliminary findings in a larger cohort is required.

64 Smad Mediated Pathways Are Active in Osteosarcoma.

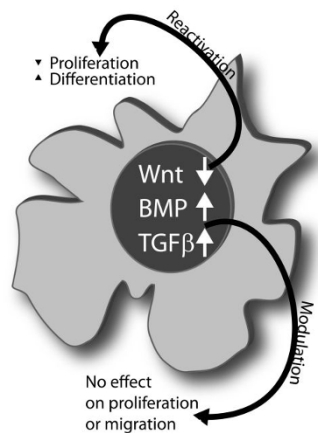
AB Mohseny, Y Cai, PCW Hogendoorn, A-M Cleton-Jansen. Leiden University Medical Center, Netherlands; School of Medicine, Shandong University, China.

Background: Conventional osteosarcoma is a highly malignant tumour mainly affecting children and adolescents. The tumour's pathogenesis is largely unknown, however the young age of onset and its metaphyseal location suggest a possible role for impaired pathways deregulating the normal rapid bone growth and renewal. Previously we showed inactivity of the Wnt/ β -catenin pathway and that its reactivation could inhibit osteosarcoma growth and promote differentiation (Cai Y et al. J Pathol. 2010 Jan; 220(1):24-33.). Here we aimed to study the role of two other important pathways in skeletogenesis — BMP and TGF β — in osteosarcoma and to record the effects of their modulation towards potential targets for therapy.

Design: Human osteosarcoma samples (n=127) and osteoblastomas (n=25) were examined for nuclear phosphorylated (p) Smad1 (BMP) and pSmad2 (TGF β) expression by immunohistochemistry. In addition the activity of both pathways was measured in 4 osteosarcoma cell lines using the BMP-responsive element (BRE)luciferase construct and the TGF β pathway responsive plasmid containing (CAGA)₁₂luciferase reporter. Furthermore BMP and TGF β pathways were modulated using BMP4, BMP inhibitor LDN-193189, TGF β -1 and TGF β inhibitor SB-431542 and the effects on proliferation and migration of the cells were recorded.

Results: Analysis of pSmad1 and pSmad2 showed high nuclear expression of both proteins in nearly 100% of the osteosarcomas at levels comparable to the osteoblastomas. This indicates that BMP and TGF β pathways are active in both bone tumour types, which is irrespective of their clinical behavior. The luciferase reporter assays confirmed that the pathways are indeed functionally active. Both pathways could be successfully modulated in the osteosarcoma cell lines; however this did not affect proliferation or migration of the cells.

Conclusions: This study shows that BMP and TGF β signaling pathways are active in high-grade central osteosarcoma cases tested, in line with the high bone resorption and vascularization seen in these tumours. Inhibiting the pathways did not affect cell proliferation or migration *in vitro*, however given the importance of interactions of tumour cells with stroma we cannot exclude that these pathways are involved in osteosarcoma genesis *in vivo*.

**65 MicroRNA-200a Expression in Synovial Sarcoma Is Related to Epithelial Differentiation.**

T Motoi, A Kumagai, A Yoshida, T Imamura, T Fukusato. Teikyo University School of Medicine, Tokyo, Japan; Tokyo University, Japan; Teikyo University Hospital, Tokyo, Japan.

Background: Synovial sarcoma (SS) is characterized by epithelial differentiation through mechanisms involving epithelial-mesenchymal transition (EMT) and mesenchymal-epithelial transition (MET). Recently, microRNA (miR)-200 family was found to play key roles in EMT/MET during tumor metastasis and invasion mainly by the regulation of E-cadherin (ECAD). To test the hypothesis that miR-200 may contribute to epithelial differentiation in SS, we examined the expression of miR-200a, a main member of miR-200 family, in SS and other sarcoma types.

Design: Formalin-fixed paraffin-embedded samples of 8 surgical cases of SS were collected, including 3 biphasic and 5 monophasic fibrous variants. For comparison, 4 malignant peripheral nerve sheath tumors, 4 solitary fibrous tumors (SFTs), 2 clear cell sarcomas, 2 dermatofibrosarcomas protuberans, 2 pleomorphic malignant fibrous histiocytomas, and 1 epithelioid sarcoma were also studied. Following total RNA extraction, the expression level of mature miR-200a was measured by quantitative RT-PCR with relative quantification calibrated by a SFT sample. SS cases were analyzed for *SYT-SSX 1/2* by RT-PCR. Epithelial differentiation was assessed by immunohistochemical expression of cytokeratin (AE1/AE3) and ECAD. Immunostaining was graded as 3+ (>=30%), 2+ (10%-<30%), 1+ (1%-<10%), and 0 (<1%).

Results: miR-200a was highly expressed in SS (fold change: 0.7-363.1, mean: 99.7) compared with other types of sarcoma (0.1-40.7, mean: 4.8) (*t*-test, *p* < 0.05). In SS, the expression level of miR-200a were correlated with the reactivity of AE1/AE3 (3+:/2/8, 2+:/1/8, 1+:/3/8, 0/2/8) and ECAD (3+:/1/8, 2+:/1/8, 1+:/1/8, 0/5/8) in spindle cell component. Two SSs with very low miR-200a level were negative for AE1/AE3 and ECAD. Four SSs harbored *SYT-SSX1* and the remaining 4 showed *SYT-SSX2*. Although

histological and genetic subtypes were not correlated with miR-200a expression status, a case of biphasic SS with predominantly epithelial component expressed high level of miR-200a.

Conclusions: The expression of miR-200a is tightly linked to epithelial differentiation in SS. miR-200a may regulate its target EMT/MET genes to induce this phenotypic change. In addition, miR-200a was differentially expressed in SS over other sarcoma types, and it can be utilized as a new diagnostic marker of SS showing true epithelial differentiation.

66 Molecular Analysis of Extra-Axial Hemangioblastoma. A Study of 6 Cases.

LA Muscarella, J Lamovec, P Parrella, N Zidar, L D'Agruma, M Bisceglia, V Guarnieri, M Coco, JC Fanburg-Smith, L Zelante, M Michal. Hospital, San Giovanni Rotondo, Foggia, Italy; Institute of Oncology, Ljubljana, Slovenia; Medical Faculty, University of Ljubljana, Slovenia; Nova Fairfax Hospital, Falls Church, VA; IRCCS "Casa Sollievo della Sofferenza" Hospital, San Giovanni Rotondo, Foggia, Italy; Charles University Medical Faculty, Plzen, Czech Republic.

Background: Extraneuraxial hemangioblastoma (e-HGB) may occur in various body organs either in the context of von Hippel-Lindau syndrome (VHL) or sporadically. Patients with VHL exhibit mutations of *VHL* gene. *VHL* gene is involved also in sporadic HGB. Only 2 cases of e-HGB have been molecularly analyzed so far, without documenting alterations in *VHL* gene, thus suggesting in one previous study that *VHL* gene may not be the causative factor of e-HGB.

Design: We report on 6 e-HGB, 4 in intraspinal/paraspinal locations and 2 in peripheral soft tissues, in 6 patients (5 females and 1 male, aged 40 to 74 years). 1 tumor was VHL-associated, 5 were sporadic. Normal and tumoral tissue samples were available from all cases. Characterization of the *VHL* gene was performed by Mutation, Fluorescent Loss of Heterozygosity (LOH) and Methylation Analysis in all cases. *Mutation analysis* searched for point mutations in the entire coding sequence and promoter region of the *VHL* gene, including the exon-intron boundaries. *LOH analysis* was performed using three microsatellite markers flanking the *VHL* gene: D3S1335, D3S1038, D3S1317. The *methylation status* in the promoter region of the *VHL* gene was determined by Methylation Specific PCR.

Results: *Mutation analysis* documented in the HGB tumor tissue of the *VHL* case (case 1) two nucleotide substitutions, the germline c.452T>A substitution in exon 2, creating the aminoacid change I151N, and the somatic c.450G>A substitution in exon 3, resulting in the aminoacid change R167Q. Most notably, a new somatic nucleotide deletion in exon 3 (c.598delA) was found in case 5, causing a frameshift with a premature predicting stop codon at position 201. *Microsatellite analysis* showed LOH in case 5 (second hit), and in case 4 and case 6 as single hit. *Methylation analysis* did not disclose promoter methylation in any tumor. No *VHL* gene alteration was demonstrated in both case 2 and case 3 by any means.

Conclusions: This is the first report of *VHL* gene alterations identified in e-HGB, confirming that the *VHL* gene is involved also in e-HGB.

67 RANKL Signaling in Bone Lesions with Osteoclast-Like Giant Cells.

K-Y Na, KY Won, RK Kalil, YW Kim, Y-K Park. Kyung Hee Medical Center, College of Medicine, Kyung Hee University, Seoul, Korea; Sarah Network of Rehabilitation Hospitals, San Paulo, Brazil.

Background: The interaction between receptor activator of NF- κ B (RANK), its ligand (RANKL), and the decoy receptor for RANKL, osteoprotegerin (OPG) performs a pivotal role in promoting osteoclast differentiation and activation leading to bone resorption. Giant cell tumors (GCT), chondroblastomas (CB), and aneurysmal bone cysts (ABC) harbor osteolytic lesions containing osteoclast-like giant cells.

Design: We selected 49 cases of GCT, 12 cases of CB, 6 cases of ABC, and 5 cases of metastatic giant cell tumors (including paired primary giant cell tumors). We evaluated RANK, RANKL, and OPG expression in giant cells of CB, GCT, and ABC via immunohistochemical methods. Additionally, the correlation between RANK, RANKL and OPG expression in these respective bone lesions was evaluated in this study.

Results: Our findings revealed that RANK, RANKL, and OPG expression in osteoclast-like giant cells differ significantly according to the disease entity (CB vs GCT vs ABC). CB showed significantly different RANK, RANKL, and OPG expression levels in comparison with GCT. And, CB evidenced significantly different RANK and OPG expression from ABC. Additionally, our findings revealed a positive correlation between RANK and OPG in CB and GCT.

Conclusions: The expression of RANK, RANKL, and OPG in osteoclast-like giant cells differ significantly according to the disease entity (CB vs GCT vs ABC). Additionally, a positive correlation was revealed between RANK and OPG in CB and GCT.

68 CD138 Expression in Osteosarcoma.

AL Nunez, GP Siegal, V Reddy, S Wei. University of Alabama at Birmingham.

Background: CD138 (syndecan-1) is a cell surface proteoglycan that is highly sensitive and specific for plasmacytic differentiation within the spectrum of hematologic disorders. Expression of syndecan-1, recognized by CD138-clustered antibodies, has also been observed in a majority of epithelial neoplasms and, rarely, soft tissue tumors. However, reactivity for CD138 in bone tumors has not been reported.

Design: A total of 27 consecutive cases of osteosarcoma were retrieved over a five-year period (January, 2005 – July, 2010) from the authors' institution. CD138 immunoreactivity was examined on cases with tissue available (n=22). Tumors were scored as positive when any unequivocal membranous staining was identified regardless of strength. Those with positive CD138 staining were subsequently stained

for immunoglobulin kappa and lambda (IgK and IgL). Similarly, a tissue microarray (TMA), consisting of 24 cases of human osteosarcoma, 24 cases of chondrosarcoma, 12 cases of giant cell tumor of bone and 9 cases of normal bone, was also evaluated.

Results: Twenty-two cases of osteosarcoma derived from 11 men and 11 women, aged 10-77 (mean age of 26.1 years), were evaluated. These included 17 cases of conventional type (13 osteoblastic, 2 chondroblastic, 1 mixed osteoblastic and chondroblastic, and 1 osteoblastic with dedifferentiated leiomyosarcoma), 2 cases of small cell type and 3 cases of parosteal osteosarcoma. Eight cases showed CD138 expression (6 conventional, 1 small cell, 1 parosteal). Two cases of osteosarcoma from the TMA (both osteoblastic) were positive for CD138. All these cases were negative for subsequent IgK and IgL staining. All cases of chondrosarcoma, giant cell tumor of bone and normal bone were negative for CD138. Thus, CD138 expression was seen in 22% of osteosarcoma cases (10/46), but not in other cases examined.

Conclusions: To our knowledge, this is the first study to examine CD138 expression in bone tumors. Our results show that CD138 reactivity for neoplastic cells in bone is not a definitive marker for plasmacytic origin. The expression of CD138 in osteosarcoma may represent a potential diagnostic pitfall, especially in a bone biopsy where the nature of the lesion needs to be determined from a limited amount of tissue. Thus, caution is required to interpret CD138+ cells from a bony lesion for which a hematologic etiology has not been established. Additionally, when plasmacytoma is in the differential diagnosis, IgK and IgL along with other appropriate markers and careful radiological correlation are needed to reach the correct diagnosis.

69 SMAD Signaling in Liposarcomas.

JE Pogoriler, AG Montag. University of Chicago Medical Center, IL.

Background: Signaling by members of the TGF β superfamily affects development of normal adipocytes. TGF β is thought to negatively regulate adipogenesis, while BMPs generally positively contribute to adipocyte development. Among other intermediates, both BMPs and TGF β receptors transduce signals by phosphorylating SMAD family members, allowing them to regulate transcription of target genes, including PPAR γ , a key regulator of adipogenesis. We hypothesized that SMAD signaling would be different among the different subtypes of liposarcomas.

Design: We constructed a liposarcoma tissue microarray that included well-differentiated (WD), de-differentiated (DD), myxoid, round-cell and pleomorphic liposarcomas, including several samples with both low and high grade components. We used immunohistochemistry to assess expression and localization of SMAD4, SMAD2/3, PPAR γ , c-jun and ask-1. Staining was scored as 0 (none), 1 (<5%), 2 (5 to 50%), or 3 (greater than 50%). For analysis purposes, scores 2 and 3 were considered positive staining.

Results: We found that nuclear SMAD4 was present in 7 of 10 DD liposarcomas but was negative in all WD liposarcomas, including the well-differentiated component of DD tumors. SMAD4 was positive in almost all myxoid, round cell, and pleomorphic liposarcomas. In contrast, nuclear SMAD2/3 was only detected in one DD tumor and was entirely absent from WD tumors. It was detected in 10/16 myxoid, 8/8 round cell and 11/12 pleomorphic liposarcomas. Within each tumor subtype there was no relationship between SMAD2/3 or SMAD4 expression and PPAR γ , c-jun and ask-1 expression.

Liposarcoma immunohistochemistry

	SMAD4	SMAD2/3	c-Jun	Ask-1	PPAR
pure WD	0/10	0/10	1/10	1/10	0/10
WD component	0/12	0/12	1/12	1/12	2/12
DD	7/10	0/10	7/10	8/10	8/10
pure myxoid	9/10	5/10	5/10	1/10	4/10
myxoid component	6/6	5/6	0/6	0/6	4/6
Round cell	8/8	8/8	2/8	3/8	6/8
Pleomorphic	11/12	11/12	8/12	10/12	8/12

Conclusions: The nuclear localization of SMAD4 and SMAD2/3 in myxoid/round cell and pleomorphic liposarcomas suggests that signaling through a TGF β receptor family member is occurring. Although SMAD2/3 was negative in DD liposarcomas, the common mediator SMAD4 was positive, suggesting that signaling through BMP or TGF β receptors is occurring, perhaps through a different receptor-activated SMAD family member.

70 Immunohistochemical and FISH Analysis of Angiosarcoma Arising in Organ Alloraft Recipients and in a Patient with Long-Standing Orthopedic Metal Implant.

BM Purgina, MA Nalesnik, K Cieply, MA Goodman, RL McGough, UNM Rao. UPMC, Pittsburgh, PA.

Background: Angiosarcoma (AS) comprises less than 1% of sarcomas and is considered high-grade. We examined a selected series of AS occurring in patients with prior organ transplants and one that occurred at the site of metal orthopedic implant and compared them with paired samples of primary and recurrent conventional AS.

Design: Paraffin blocks from 15 patients with AS were retrieved from archived files at our institution. 10 had recurrent AS, 4 had metastases. Follow-up clinical data was available for 10 patients including two AS in organ transplant recipients (one also had NF1), and AS of the proximal tibia containing an orthopedic metal implant for more than 25 years. The rest of AS were primary in subcutaneous soft tissue. We categorized AS histologically as low grade and epithelioid. Immunohistochemistry included antibodies for at least 3 vascular markers, cytokeratins, ckit, Ki67, and in older and/or immunocompromised patients, HHV8 and EBV. Paired samples of primary and metastatic AS in 4 patients, including a transplant patient were selected for FISH analysis for EGFR using LSI EGFR/CEP7 dual-color probe (7p12).

Results: All cases demonstrated positivity with one or more vascular markers. The 4 cases of metastatic AS demonstrated epithelioid features. Low-grade AS without epithelioid features were positive for more than two vascular markers, and all were

negative for cytokeratins. Epithelioid AS were focally positive for CD31, variable for the other vascular markers and focally positive with cytokeratins. Ki67 positivity ranged from 5% in low-grade AS to over 90% in epithelioid AS. HHV8, EBV and ckit were negative. None of the 4 cases demonstrated EGFR amplification but 4 of the 6 samples demonstrated hyperploidy in the range of 13-36%. Epithelioid AS had much more aggressive course with multiple recurrences, metastatic disease and proved fatal in three patients including the patient with metal-associated AS.

Conclusions: AS with epithelioid features had fewer positive vascular markers, possibly reflecting a lack of differentiation. There were no differences in pattern of immunoreactivity with post transplant and conventional AS. Primary bones AS associated with metal orthopedic implants are exceedingly rare. EGFR hyperploidy was likely related to copy number gains of chromosome 7. Even though AS is a rare tumor, the aggressive and rapidly lethal course warrants continued investigation in order to identify new therapeutic targets.

71 Molecular Alteration Implicated in Malignant Transformation of Peripheral Nerve Sheath Tumors (PNST): A Window to New Therapeutic Approaches.

C Romagosa, C Serrano, S Simonetti, J Hernandez-Losa, S Bague, R Orellana, T Moline, R Somoza, S Ramon y Cajal. Hospital Vall d'Hebron, Barcelona, Spain; Hospital de Sant Pau, Barcelona, Spain; Hospital Parc Taulí, Sabadell, Spain.

Background: Benign (BPNST) and malignant (MPNST) peripheral nerve sheath tumors are found to be either sporadic or related to neurofibromatosis (NF). Ras-Raf-MAPK pathway activation has already been described in both groups. While NF1 and NF2 loss of function leads to oncogenic Ras signalling in NF associated tumors, other mechanisms in the sporadic setting remain unknown. Somatic BRAF mutations are involved in the pathogenesis of a wide variety of cancers by triggering the Ras-Raf-MAPK pathway, which in turn constitutes a target for new treatments. However, activation of the Ras-Raf-MAPK cascade has been also described in benign tumors, indicating that these are initial events in tumoral transformation. P16 and PTEN downregulation have been described as critical events in malignant transformation in other tumours initiated by activation of the Ras-Raf-MAPK pathway. The aim of this study was to investigate the implication of BRAF V600E mutations and P16 or PTEN downregulation in sporadic and NF-associated nerve sheath tumors.

Design: BRAF exon 15 PCR amplification and sequencing was done in 18 schwannomas (1 NF, 16 sporadic and 1 unknown), 16 neurofibromas (5 NF and 9 sporadic) and 19 MPNST (9 NF, 8 sporadic and 2=unknown). cDNA was obtained from formalin-fixed and paraffin-embedded tissue in all cases. Moreover, immunohistochemical staining was done in all the cases for p16 (V-Kit CINTec, MTM), and for PTEN (Anti-hu PTEN (6h2.1), Cascade) in a subgroup of 12 Schwannomas, 12 Neurofibromas and 17 MPNST.

Results: BRAF V600E mutations were detected in 3/16 (18.8%) sporadic schwannomas and 1/8 (12.5%) sporadic MPNST. No BRAF mutation were observed in any neurofibroma or any NF associated lesion. PTEN loss was observed in 5/17 (29.5%) of MPNST and 0/24 (0%) BPNST. Differences in p16 expression were observed between MPNST (8.95+/-16.78) and BPNST (45.43+/-27.77) (p=0.0001).

Conclusions: Our findings confirm the presence of BRAF V600E mutations in sporadic Schwannomas and MPNST but not in Neurofibromas. These data suggest that BRAF V600E mutation might arise as a key event in cell growth and development of a subgroup of BPNST and MPNST non-related to NF. Moreover, our data support the hypothesis that p16 and PTEN loss are critical events in malignant transformation of MPNST. Together, our results open new avenues to test and develop upcoming treatments for these group of tumors

72 Malignant Fibrous Histiocytoma and Fibrosarcoma of Bone in 2011: What's New?

S Romeo, JVMG Bovee, I Carraretto, R Tirabosco, C Natali, HM Kroon, L Zanatta, R Scioc, F Mertens, N Athanasou, M Alberghini, PCW Hogendoorn, AP Dei Tos. Treviso Regional Hospital, Treviso, Italy; Leiden University Medical Center, Netherlands; Royal National Orthopaedic Hospital, London, United Kingdom; Rovigo Regional Hospital, Rovigo, Italy; Leuven University, Netherlands; Lund University Hospital, Lund, Sweden; Nuffield Orthopaedic Center, Oxford, United Kingdom; Rizzoli Orthopaedic Institute, Bologna, Italy.

Background: Malignant fibrous histiocytoma (MFH) and fibrosarcoma (FS) of bone are rare primary malignant bone tumors and contentious entities. Cases diagnosed as bone MFH and FS were retrieved from the archives of 5 bone tumor referral centers and reviewed to determine whether recent advances in immunohistochemistry together with new tumor classification allowed for reclassification and identification of histologic subgroups associated with distinct clinical behavior.

Design: Tumors originally diagnosed as MFH (n= 51) and FS (n=9) of bone were collected within EuroBoNeT, a European Commission-funded network of excellence for the study of the pathology and biology of bone tumors. A panel of immunostains was applied to each case including: SMA, desmin, H-caldesmon, CKAE3-1, CD31, CD34, CD68, CD163, CD45, S100, and EMA. Additional FISH and immunohistochemical analyses were performed, when appropriate, to confirm/reject alternative diagnoses. All cases were reviewed by 6 experienced bone pathologists; in discrepant cases a consensus was reached at a joint microscopy session.

Results: After morphologic, immunohistochemical and radiologic analyses, seven cases were reclassified as leiomyosarcoma, one as spindle cell rhabdomyosarcoma, three as myxofibrosarcoma and five as osteosarcoma. Among the remaining 44 cases we identified 5 subgroups. Four were reclassified as spindle cell sarcoma not otherwise specified and their morphology corresponded well with the previous description for bone FS. Seven cases were reclassified as undifferentiated pleomorphic sarcoma (UPS) and 10 as UPS with incomplete myogenic differentiation, due to positivity for at least one

myogenic marker. Among the remaining 23 cases we identified a further two recurrent morphologic patterns: 8 cases demonstrated a myoepithelioma-like phenotype, while 15 cases displayed a myofibroblastic phenotype.

Conclusions: In a substantial number of cases the diagnoses were changed due to new immunohistochemical markers and revised diagnostic criteria. Five subgroups were identified in the remaining cases. In parallel to previous data on soft tissue MFH, identification of these subgroups may be prognostically relevant.

73 Claudin-5: A Novel, Highly Sensitive and Specific Endothelial Marker.

W Shon, LA Popp, AL Folpe. Mayo Clinic, Rochester, MN.

Background: Claudin-5, a member of the claudin family of tight junction-associated proteins, is thought to be chiefly expressed in endothelial cells under normal states. Although claudin-5 expression has been recently observed in rare cases of carcinoma of pancreatic and lung origin, antibodies to claudin-5 have not been systematically examined as diagnostic reagents. Prompted by a recent study showing claudin-5 expression in canine angiosarcomas, we studied claudin-5 expression in angiosarcomas, non-endothelial mesenchymal tumors, carcinomas, and normal tissues.

Design: Formalin-fixed, paraffin embedded whole sections (20 angiosarcomas, 1 epithelioid hemangioendothelioma, 39 non-endothelial mesenchymal tumors, 2 mesotheliomas, 2 melanomas, 11 carcinomas of various sites, and 2 germ cell tumors) and 2 tissue microarray sections (1 with 146 pancreatic adenocarcinomas; 1 with 42 cases each of lung, ovarian, and pancreatic carcinoma as well as normal tissues) were immunostained for claudin-5 (polyclonal, 1:100, Abcam) using heat-induced epitope retrieval and the Dako EnVision detection system. Membranous immunoreactivity was scored as negative (<5%), 1+ (5-25%), 2+ (26-50%), 3+ (>51%). Appropriate controls were employed.

Results: Claudin-5 expression was seen in 19/20 (95%) angiosarcomas (1+: 5, 3+: 14) and in the case of epithelioid hemangioendothelioma (2+). All non-endothelial mesenchymal tumors were claudin-5 negative. Amongst non-mesenchymal tumors, claudin-5 expression was seen only in carcinomas of pancreatic (11/146, 8%) and gastric (2/2, 100%) origin, and in a case of yolk sac tumor. In normal tissues, claudin-5 expression was confined to endothelial cells, gastric foveolar cells, colonic surface mucosa, and placental trophoblast. The overall sensitivity and specificity of claudin-5 expression for endothelial neoplasms was 95% and 93%, respectively. Claudin-5 immunostaining was notably "clean", with little or no non-membranous positivity.

Conclusions: The sensitivity and specificity of claudin-5 immunohistochemistry for those endothelial neoplasms tested to date (primarily angiosarcoma) rivals or exceeds those of established endothelial markers (e.g., CD31, CD34, Fli-1, vWF). On-going study of additional malignant, borderline and benign vascular tumors and malformations, as well as additional non-endothelial tumors, should further clarify potential diagnostic roles for this novel endothelial marker. We have also confirmed prior reports of claudin-5 expression in a subset of pancreatic adenocarcinomas, a finding that may be potentially of value in the distinction of such tumors from carcinomas of other primary sites.

74 Transducin-Like Enhancer of Split-3 (TLE3) Is Differentially Expressed in Angiosarcomas (AS) of Sporadic Cutaneous, Sporadic Soft Tissue/Visceral and Post-Irradiation Types: A Study of 100 Cases.

W Shon, DT Ross, RS Seitz, RA Beck, BZ Ring, SH Okuno, AL Folpe. Mayo Clinic, Rochester, MN; Clariant Inc., Aliso Viejo, CA.

Background: TLE3, a member of the transducin-like enhancer of split (TLE) family of proteins, is a transcriptional repressor that interacts with the Notch/WNT pathway. Recently, expression of TLE3 has been associated with improved outcome in breast cancer patients treated with taxanes. As taxanes are also commonly used for the treatment of AS, we investigated the frequency of TLE3 expression in a large series of these sarcomas.

Design: All available materials from 100 AS (38 cutaneous (AS-C), 49 soft tissue/visceral (AS-STV), and 13 post-irradiation (AS-PRT) were retrieved. Follow-up (F/U) was obtained. Formalin-fixed, paraffin-embedded sections were immunostained for TLE3 (monoclonal, 1:2000, Clariant) using heat-induced epitope retrieval and the Bond polymer refine detection system. Nuclear immunoreactivity was scored as "negative" (<5% positive cells) and "positive" (\geq 5% positive cells). Appropriate controls were employed. Fisher's exact and Kaplan-Meier tests were performed.

Results: Cases occurred in 51F and 49M (median age 64 yrs; range 3 mos-90 yrs). AS-C most often involved the head/neck, AS-STV occurred in a variety of soft tissue/visceral locations, AS-PRT involved breast skin. Overall, 33/100 (33%) AS were TLE3+. TLE3 expression was strongly associated with AS subtype, with expression in 0/38 (0%) AS-C, 29/49 (59%) AS-ST and 4/13 (31%) AS-PRT ($p < 0.001$). TLE3 expression was significantly more common in poorly differentiated (epithelioid or spindle) AS (24/56, 43%) vs well-differentiated (vasoformative) AS (9/44, 20%). Clinical F/U was available on 86/100 (86%) patients (31 dead of disease, 7 dead of other causes, 24 dead of unknown cause, 24 alive without disease; median 65 mos, range 35-250 mos). 20 patients were known to have been treated with a taxane. No differences in survival were seen in TLE3+ vs TLE3- AS, whether treated with a taxane or not.

Conclusions: Expression of TLE3 is present in up to one-third of AS, most often poorly differentiated, non-vasoformative AS-STV. Surprisingly, TLE3 expression is not seen in AS-C, possibly reflecting the different pathogenesis (sun exposure) of this subset of AS. Alternatively, TLE3 expression could represent a late event in AS, accounting for its more frequent expression in generally larger and more poorly differentiated AS-STV. Although we did not find a statistically significant relationship between TLE3 expression and survival or taxane response, these issues should be investigated in a larger, prospective study.

75 Clinicopathological, Immunohistochemical, Ultrastructural and Molecular Analysis of Clear Cell Sarcoma (CCS)-Like Tumor of the GI Tract.

DL Stockman, M Miettinen, D Spagnolo, H Dominguez, V Adsay, P Chou, P vanTuinen, B Amanuel, S Suster, EV Zambrano. Medical College of Wisconsin, Milwaukee; Armed Forces Institute of Pathology, Washington, DC; QEII Medical Centre, Nedlands, Western Australia, Australia; Cancer Institute of Mexico, Mexico City, Mexico; Emory University Hospital, Atlanta, GA; Children's Memorial Hospital, Chicago, IL.

Background: CCS of soft parts is a rare soft tissue tumor, defined by S100 positivity, melanocytic markers, ultrastructural melanosomes and specific chromosomal abnormalities. A GI tumor, possessing the same chromosomal abnormalities, but with different morphologic, immunophenotypic, ultrastructural and behavioral characteristics, has been described and designated CCS of GI tract (CCS-GI).

Design: 15 cases of CCS-GI were analyzed for the clinical, histopathological, immunohistochemical and molecular features.

Results: 8 female and 7 male patients (mean age: 43; range: 17-77); all de novo neoplasms involving small intestine (10), stomach (3), and colon (2), with solid, nested, trabecular/ribbon-like, pseudoalveolar, pseudoglandular, pseudopapillary, and fascicular patterns featuring predominantly epithelioid cytologic features, ranging from small to fusiform. Nucleoli were prominent. Mitotic activity was high. Osteoclast-like giant cells were identified in most cases. All cases showed vimentin, S100, and SOX10 expression. Synaptophysin was detected in 7/13, CD56 in 4/7, NSE in 4/8. All cases were negative for GIST (DOG1, CD117, CD34) and melanocytic (HMB45, MelanA, Tyrosinase) markers. MITF showed focal (<1%) weak positivity in 2 cases. AE1/AE3, SMA and desmin were negative in all cases. Ultrastructural analysis of 5 cases yielded synapse-like structures, primitive gap junctions, dense core granules and no identifiable melanosomes or premelanosomes. Ewing sarcoma breakpoint region 1 (EWSR1), CREB1 and ATF1, were studied by break-apart FISH in 10 cases showing EWSR1-ATF1 t(12;22) (6), EWSR1-CREB1 t(2;22) (1), extra EWSR1 copies (1), and EWSR1-? t(?;22) (2). Follow-up data showed death 3-108 months (mean: 37) after initial surgery (7), alive with disease (2), and no evidence of disease (1).

Conclusions: This study shows that CCS-GI follows a neuroectodermal line of differentiation, displaying S100, SOX10, Synaptophysin, and NSE positivity, with synapse-like structures and dense core granules at the ultrastructural level, for which we propose the term gastrointestinal neuroectodermal tumor (GNET).

76 TFE3-Positive Perivascular Epithelioid Cell Tumor as a Distinct Entity: Morphological, Immunohistochemical, and Molecular Analyses.

M Tanaka, K Kato, K Gomi, M Yoshida, K Kurosawa, H Kigasawa, Y Ohama, G Taylor, Y Tanaka. Kanagawa Children's Medical Center, Yokohama, Japan; Ibaraki Children's Hospital, Mito, Japan; Hospital for Sick Children, Toronto, Canada.

Background: Perivascular epithelioid cell tumors (PEComas) are mesenchymal tumors composed of perivascular epithelioid neoplastic cells that are immunoreactive for melanocytic and muscle markers. Nine cases of PEComa with TFE3 immunoreactivity (TFE3+ PEComa) are reported in the literature. Recently, we reported a case of PEComa with a *SFPQ-TFE3* gene fusion, arising in the sigmoid colon, which was the first report confirming a specific fusion gene in PEComa (Am J Surg Pathol. 2009;33:1416). In the present study, four cases of TFE3+ PEComa, including two previously reported cases (Pediatr Dev Pathol 2005;8:98, and Hum Pathol 2010;41:768), a newly identified case, and our reported case, were examined to clarify the characteristic features of TFE3+ PEComa.

Design: Two of the TFE3+ PEComas examined arose in the orbit, one in the sigmoid colon, and one in the uvea. A histological review, immunohistochemical (IHC) analysis of TFE3, MITF, gp100, melan-A, and smooth muscle actin (SMA), and the detection of fusion genes with RT-PCR or FISH analyses were performed.

Results: The most striking histological feature was melanin pigmentation, which was observed to various degrees in all the tumors examined. On IHC analysis, all tumors showed immunoreactivity for TFE3 and gp100, but were not immunoreactive for melan-A or MITF. The sigmoid colon tumor was negative for SMA, whereas the other three tumors were at least partially positive for it. On FISH analysis, split signals for *TFE3* were detected in all four tumors. On RT-PCR analysis, a *NONO-TFE3* fusion gene was confirmed in one orbital tumor.

Conclusions: All four TFE3+ PEComas examined had common characteristic histological features (melanin pigmentation) and immunohistological features (positive for gp100 and negative for melan-A and MITF). *SFPQ* and *NONO* are closely related pre-mRNA splicing factors, and *SFPQ* and *NONO-TFE3* are not common among *TFE3*-related fusion genes. It was interesting that these uncommon fusion genes were detected in this study. Our results suggest that at least a certain subgroup of TFE3+ PEComas constitutes an immunohistochemically and cytogenetically distinct entity among the PEComa family of tumors.

77 Prognostic and Potentially Therapeutic Implications of MTAP Depletion in Myxofibrosarcoma.

J-W Tsai, F-M Fang, C-F Li, T-J Chen, Y-H Wang, H-Y Huang. E-Da Hospital, Kaohsiung, Taiwan; Chang Gung Memorial Hospital, Kaohsiung, Taiwan; Chi-Mei Hosp., Tainan, Taiwan; Institute of Biomedical Sciences, National Sun Yat-Sen University, Kaohsiung, Taiwan; Institute of Biosignal Transduction, NCKU, Tainan, Taiwan.

Background: Myxofibrosarcoma (MFS) is genetically complex and remains obscure in molecular determinants of clinical aggressiveness. A large-scale genomic study recently reported deletions of classical tumor suppressor genes (TSGs), *CDKN2A/CDKN2B*, at 9p21.3, while other potential TSGs on chromosome 9 are less understood in MFS.

Design: Genome-wide 385K array comparative genomic hybridization (aCGH) was profiled for 12 tumors and 2 cell lines (OH931, NMFH-1) of MFS, with special attention to potential TSGs on 9p. Three MFS cell lines (OH931, NMFH-1, NMFH-2) were subjected to immunoblotting and quantitative PCR (qPCR) assays, respectively, to analyze the MTAP protein expression and gene dosage relative to diploid dermal fibroblasts. These cell lines were also examined by XTT assay to evaluate their cell viability upon L-alanine treatment. An independent cohort of primary MFS on tissue microarrays were immunostained for MTAP protein, yielding 87 cases with assessable results that were further correlated with clinicopathological variables and patient survival.

Results: aCGH identified recurrent DNA deletions spanning 90 genes on 9p and 116 genes on 9q. *MTAP* and *CDKN2A/CDKN2B* at 9p21.3 were deleted in 5 and 6 cases, respectively, with 1 case homozygously co-deleted at both loci. As for *MTAP*, OH931 and NMFH-2 cells showed neither detectable gene by qPCR nor protein expression by immunoblotting, while NMFH-1 had preserved gene and protein of *MTAP*, corresponding to aCGH findings. As compared to NMFH-1 cells ($IC_{50} \sim 100$ uM), *MTAP*-depleted OH931 ($IC_{50} \sim 50$ uM) and NMFH-2 ($IC_{50} < 1$ uM) cells were more susceptible to L-alanine, a *MTAP*-directed agent inhibiting de novo AMP synthesis. There were 32 of 87 cases showing loss of *MTAP* protein immunoreactivity, which, albeit not related to clinicopathological variables, were independently associated with disease-specific survival ($p=0.014$, $RR=4.020$) alone and with metastasis-free survival ($p=0.0318$, risk ratio $[RR]=2.527$), along with higher grades.

Conclusions: *MTAP* protein deficiency, present in 37% of primary MFS, independently portends worse prognosis, while its underlying inactivating mechanisms are currently being elucidated by both methylation-specific PCR and qPCR. *MTAP*-depleted MFS cells are more susceptible to L-alanine. These findings indicate the potentiality of *MTAP* as prognostic and/or therapeutic biomarker of MFS.

78 Poorly Differentiated Chordomas. Diagnostic Utility of Immunohistochemistry for Brachyury and SMARCB1/INI1.

H Vogel, JK McKenney, CD Bangs, MSB Edwards, PG Fisher, K Callahan, M Gokden, BC Mobley. Stanford University, Palo Alto, CA; University of Arkansas, Little Rock.

Background: Chordomas in pediatric patients are more likely to display unusual histological features and aggressive behavior. We noted the absence of SMARCB1/INI1 expression by immunohistochemistry while retaining brachyury expression, a marker of notochordal differentiation, in a poorly differentiated chordoma of the sacrum in an 11 year old female.

Design: We examined 3 additional poorly differentiated chordomas of the clivus, 10 typical chordomas, and 8 atypical teratoid/rhabdoid tumors (AT/RTs) by immunohistochemistry for brachyury and SMARCB1/INI1 in order to test the utility of this immunophenotype in identifying poorly differentiated chordomas. Fluorescence in situ hybridization for markers on 22p was performed in all cases.

Results: The three additional cases were of a 7 year old male, 22 month old female, and 3 year old female. The index case, 7, and 3 year old patients were dead of disease within 12 months of diagnosis. The 22 month old female was alive with recurrent disease 12 months postoperatively. Poorly differentiated chordomas were composed of mitotically active epithelioid cells with moderately pleomorphic nuclei and prominent nucleoli. Foci of necrosis were evident for each case. Vacuolated cells were generally unapparent. All chordomas including the poorly differentiated examples were brachyury immunopositive, while all eight AT/RTs were negative for the marker; among the chordomas, only the poorly differentiated examples were SMARCB1/INI1 immunonegative, as were all of the AT/RTs. The poorly differentiated chordomas showed diffuse cytoplasmic pankeratin reactivity. Nuclear and cytoplasmic S-100 staining was observed focally in three cases and was negative in the fourth. FISH analysis using markers to chromosome 22p distal to the SMARCB1/INI1 locus indicated heterozygous deletions in three of the cases.

Conclusions: Poorly differentiated chordomas retain brachyury expression but commonly show absent SMARCB1/INI1 expression, thus can be distinguished from AT/RTs and other neoplasms by the identification of nuclear brachyury expression. Our findings suggest the loss of SMARCB1/INI1 in the subset of chordomas with aggressive features.

79 Frequency of MDM2 Amplification in Malignant Peripheral Nerve Sheath Tumors: Non-Correlation with Tumor Grade, Cellularity and MIB1 Proliferation Index.

ML Wallander, LJ Layfield. ARUP Institute for Clinical and Experimental Pathology, Salt Lake City, UT; University of Utah School of Medicine and ARUP Laboratories, Salt Lake City.

Background: The p53 tumor suppressor gene is inactivated by a variety of mechanisms including interaction with the MDM2 oncoprotein. MDM2 is known to be abnormally upregulated in a variety of human neoplasms secondary to gene amplification. Assessment of MDM2 amplification is clinically most useful for the separation of lipomas from atypical lipomatous neoplasms/well differentiated liposarcomas. MDM2 is amplified in liposarcomas but not in lipomas. MDM2 amplification occurs in approximately 7% of all human neoplasms with the highest frequency of amplification being found in soft tissue tumors (20%), osteosarcomas (16%) and esophageal carcinomas (13%). Early studies have indicated that MDM2 is not amplified in malignant peripheral nerve sheath tumors.

Design: Sixteen malignant peripheral nerve sheath tumors and five schwannomas were obtained from the files of the Department of Pathology. These cases underwent fluorescence in situ hybridization analysis for the presence of MDM2 amplification. For each malignant peripheral nerve sheath tumor, assessments were made for cellularity (low or high), percentage of cells staining positively for p53 and percentage of cells staining with MIB-1.

Results: Three of sixteen (19%) malignant peripheral nerve sheath tumors demonstrated amplification of the MDM2 gene. None of the schwannomas demonstrated MDM2 amplification. Malignant peripheral nerve sheath tumors associated with MDM2 amplification demonstrated a MIB1 proliferation index of 39% or greater and all three amplified cases demonstrated a high percentage of cells staining for p53 (18%, 32% and 55%).

Conclusions: Prior studies have failed to demonstrate MDM2 amplification in malignant peripheral nerve sheath tumors. Our study demonstrated that approximately 19% of malignant peripheral nerve sheath tumors display amplification of the MDM2 gene. Malignant peripheral nerve sheath tumors demonstrating MDM2 amplification had a higher than average MIB1 proliferation index and a higher than average percentage of cells staining for p53. MDM2 amplification may represent a method for inactivation of p53 in a subset of malignant peripheral nerve sheath tumors and may result in an increased proliferation index.

80 BCL-6 Expression in Mesenchymal Tumors: An Immunohistochemical and Fluorescence In Situ Hybridization Study.

MP Walters, AL Folpe. Mayo Clinic, Rochester, MN.

Background: The BCL-6 proto-oncogene encodes a transcriptional repressor protein, best known for its regulatory role in germinal center lymphocyte differentiation and survival. Among normal tissues, BCL-6 expression at a level detectable by immunohistochemistry (IHC) is typically confined to germinal center B-cells and a subpopulation of T-helper cells. Very little is known about BCL-6 expression in mesenchymal tissues. Prompted by a recent case of solitary fibrous tumor (SFT) showing strong BCL-6 immunoreactivity, we examined a series of SFT and other spindle cell mesenchymal tumors for BCL-6 expression.

Design: Formalin-fixed, paraffin-embedded tissue sections from 55 mesenchymal tumors [26 SFT (19 benign/uncertain, 7 malignant), 6 synovial sarcomas (SS), 5 GIST, 5 MPNST, 5 leiomyosarcomas (LMS), 4 desmoid tumors (DT), 4 perineuriomas (PN)] were immunostained for BCL-6 using a commercial antibody and the Dako Envision system. Cases were scored as "negative", "1+" (5-25% positive), "2+" (26-50% positive) and "3+" (>51% positive). Only nuclear immunoreactivity was considered positive. Appropriate controls were employed. Six BCL-6 positive SFT were also tested for BCL-6 gene rearrangement/amplification by FISH, using previously published methods.

Results: Nuclear expression of BCL-6 was seen in 13/26 SFT (1+ 7, 2+ 6), 5/5 LMS (2+ 3, 3+ 3), 5/6 SS (1+ 4, 2+ 1), 1/5 GIST (2+), 1/5 MPNST (2+), 1/4 PN (1+), and 0/5 DT. BCL-6 expression was significantly more frequent in malignant (6/7) as compared with benign/uncertain SFT (6/19) ($p=0.02$, Fishers Exact Test). FISH for BCL-6 rearrangement/amplification was negative in all tested cases.

Conclusions: In this, the first study to date of BCL-6 expression in mesenchymal tumors, we have observed strong (2-3+) BCL-6 expression in 50% or more of SFT, SS, and LMS, and in a lesser percentage of GIST, MPNST and PN. Given these findings, it is doubtful that there is a role for BCL-6 IHC in the differential diagnosis of spindle cell tumors. Significantly more frequent expression of BCL-6 in malignant as compared with benign/uncertain SFT suggests that abnormalities in the BCL-6 signalling pathway may contribute to malignant transformation in at least some mesenchymal tumors. Based on our (limited) FISH data, it is unlikely that BCL-6 expression in mesenchymal tumors is due to BCL-6 gene amplification or rearrangement. With the development of new therapeutic agents targeting the BCL-6 pathway, IHC for BCL-6 may potentially be of value in predicting response to such agents in patients with aggressive or unresectable disease.

81 Fusion of Dynactin 1 (DCTN1) to ALK in Inflammatory Myofibroblastic Tumor.

X Wang, C Krishnan, E Nguyen, KJ Mayer, JL Oliveira, JE Yi, P Yang, MJ Yaszenski, A Maran, MR Erickson-Johnson, AM Oliveira. Mayo Clinic, Rochester, MN; Dells Children's Medical Center of Central Texas, Austin; Mayo Medical School, Rochester, MN; Mayo Clinic, Rochester, MN.

Background: Inflammatory myofibroblastic tumor (IMT) is an uncommon mesenchymal neoplasm that usually occurs in younger patients. Approximately 40-50% of cases show genomic rearrangements of the *ALK* locus with the formation of fusion genes, most commonly *TPM3* and *TMP4*. Herein, we report the identification of a novel fusion of the cytoskeleton dynactin 1 gene (*DCTN1*) to *ALK* in IMT.

Design: Histologic review, immunohistochemical evaluation for ALK (Dako, Carpinteria, CA) and cytogenetic G-banding analysis were performed using standard techniques. Fluorescence in situ hybridization (FISH) using a commercially available *ALK* probe (Vysis Inc., Downers Grove, IL, USA) was performed on metaphase and interphase cells. RNA was extracted from cultured tumor cells using standard protocols. Identification of the *ALK* partner gene was carried out using 5'-rapid amplified cDNA end (5'-RACE) PCR, and confirmed by specific RT-PCR and direct sequencing in triplicate experiments.

Results: A 7-year old female presented with a posterior neck mass measuring 6 cm in greatest dimension. Histologic and immunohistochemical analysis showed a bland spindle cell neoplasm that weakly expressed ALK in a finely granular cytoplasmic pattern. Cytogenetic studies revealed the following karyotype: 46,XX,der(2)t(2;12)(p23;q11)[18]/46,idem,der(11)t(3;11)(p11;q23)[2]. Molecular cytogenetic analysis demonstrated rupture and inversion of the centromeric *ALK* probe on chromosome 2. 5'-RACE PCR identified the in-frame fusion of the exon 16 of *DCTN1* on chromosome 2 to the exon 20 of *ALK*. Specific RT-PCR and direct sequencing confirmed the fusion of *DCTN1-ALK*.

Conclusions: In this study, a novel *DCTN1-ALK* fusion was identified in IMT. *DCTN1* encodes for dynactin 1, a highly expressed 150 kD cytoskeleton protein that binds to the microtubule protein dynein. The predicted structure of this novel fusion retains the cytoplasmic associated protein (CAP)-glycine and oligomerization domains of *DCTN1*,

and the tyrosine kinase domain of *ALK*. The *ALK* immunostaining pattern is consistent with the predicted structure of the novel chimeric protein.

82 Identification of a Novel, Recurrent *HEY1-NCOA2* Fusion in Mesenchymal Chondrosarcoma Based on a Genome-Wide Screen of Exon-Level Expression Data.

L Wang, T Motoi, R Khanin, N Socci, A Olshen, F Mertens, J Bridge, P Dal Cin, EJ Rushing, J Fanburg-Smith, C Antonescu, M Hameed, M Ladanyi. Memorial Sloan-Kettering Cancer Center, New York, NY; Lund University Hospital, Lund, Sweden; University of Nebraska Medical Center, Omaha; Brigham & Women's Hospital, Boston, MA; AFIP, Washington, DC; Inova Fairfax Hospital, Falls Church, VA.

Background: Cancer gene fusions that lead to the formation of a chimeric protein are often characterized by an intragenic discontinuity in the expression levels of the exons that are 5' or 3' to the fusion point in one or both of the fusion partners. Based on this, we developed an unbiased, genome-wide bioinformatic screen for this feature of gene fusions using Affymetrix Exon array expression data and report here its successful application in the identification of a new, recurrent sarcoma gene fusion.

Design: We studied 87 samples from 13 tumor cell lines and 74 tumor tissues, including 46 samples with different known gene fusions confirmed by RT-PCR. RNAs were hybridized to Affymetrix Exon 1.0 chips, providing coverage of essentially all protein-coding genes. A custom data analysis pipeline, the "Fusion Score (FS) model", was developed to score genes for intragenic changes in expression. The FS was computed for each gene in each sample. Genes with high FS in normal control samples were excluded, while the remaining genes with "true" high FS were considered as candidates for further investigation.

Results: The FS model data analysis pipeline was trained using the data from the 46 cases with known fusions. In the remaining 41 tumor samples of various histologies (including 28 mesenchymal or embryonal tumors) with possible unknown gene fusions, the FS model generated a list of 606 candidate genes showing, in one or more samples of a given histology, significant intragenic changes in expression not seen in control samples. The transcription factor gene *NCOA2* was one of the candidates identified in a mesenchymal chondrosarcoma. 5' RACE was performed, and a novel *HEY1-NCOA2* fusion was isolated, representing an in-frame fusion of *HEY1* exon 3 to *NCOA2* exon 13, encoding a predicted protein including the *HEY1* DNA binding domain and the *NCOA2* activation domain. Another 8 mesenchymal chondrosarcoma cases were screened, and the same *HEY1-NCOA2* fusion was identified in 2 more cases.

Conclusions: The present approach is able to identify fusion transcripts without any prior knowledge of the genetics of a given case or tumor type. The novel *HEY1-NCOA2* fusion is the first recurrent gene fusion identified in mesenchymal chondrosarcomas.

83 Genetic Testing in the Evaluation of Low-Grade Fibromyxoid Sarcoma.

MD Weindel, W-L Wang, E Demicco, HL Evans, VS Hernandez, TT Ton, AJ Lazar, D Lopez-Terrada. Baylor College of Medicine/Texas Children's Hospital, Houston, TX; The University of Texas M.D. Anderson Cancer Center, Houston.

Background: Low-grade fibromyxoid sarcoma (LGFMS) is a mesenchymal neoplasm with relatively bland histology, nonetheless 5-10% of cases metastasize. A balanced translocation, t(7;16)(q32-q34;p11), fusing the 5' portion of *FUS* to the 3' portion of *CREB3L2* or in a minority of tumors *CREB3L1* on chromosome 11p11 is characteristic. A subset of cases harbor a supernumerary ring chromosome with gain of material from chromosomes 7 and 16, possibly associated with a more aggressive clinical behavior. We examined 26 cases of LGFMS for the presence of a *FUS* rearrangement by FISH, and for *FUS/CREB3L2*, *FUS/CREB3L1* fusion transcripts by RT-PCR. Additionally, *FUS* copy number was examined by FISH. The findings were correlated with the clinical and pathological features.

Design: Available FFPE tissue from 26 LGFMS cases from 1994-2010 were retrieved from the pathology files of our institutions and tabulated with clinical information. FISH analysis using unstained slides was performed using a commercially available *FUS* break-apart probe on all cases. *FUS/CREB3L2* and *FUS/CREB3L1* RT-PCR was performed as previously described (Guillou *et al.*) using tissue blocks (12 cases) and unstained slides (13 cases). Amplicons from all positive cases were sequenced by the Sanger method.

Results: The age of presentation ranged from 4 to 85 years (median, 37) with a slight male predominance. The location varied from extremities to trunk; 3 cases metastasized. FISH detected a *FUS* rearrangement in 20/22 informative cases. Of these, 3 cases showed an extra rearranged copy of *FUS*. None of these 3 cases metastasized; however 2 cases were locally aggressive. Of the 25 cases evaluated by RT-PCR, 18 cases were excluded due to poor RNA quality, and 6 of 7 informative cases were positive for *FUS/CREB3L2* with sequence confirmation. RT-PCR and FISH showed complete correlation (n = 5).

Conclusions: A *FUS* gene rearrangement was found in most cases. Locally aggressive tumor behavior was noted in 2/3 cases carrying an extra copy of *FUS*, raising the possibility of an association with a more aggressive clinical phenotype. In addition to being useful to evaluate *FUS* copy number, FISH was found to be more often informative to detect *FUS* re-arrangements than RT-PCR, when testing archival FFPE tumor samples.

84 Rosai-Dorfman Disease: Another Possible IgG4 Sclerosing Disease?

DB Wimmer, YH Ko, J Huh, BH Park, A Lewis, S Shen, AG Ayala, JY Ro. The Methodist Hospital, Weill Medical College of Cornell University, Houston, TX; Sam Sung, Seoul, Korea; Asan Medical Center, Seoul, Korea.

Background: Rosai-Dorfman disease (RDD) is a rare non-malignant histiocytic proliferation of unknown etiology. IgG4 sclerosing disease is a recently described

entity, known to occur in a variety of anatomic sites, and characterized by sclerosis in the presence of an IgG4-positive plasma cell infiltration. Recent reports have examined the possible link between Rosai-Dorfman disease and IgG4 related sclerosing disease. We present 7 cases of RDD that have features of IgG4 related sclerosing disease and attempt to forge a relationship between the two entities.

Design: We reviewed 7 cases of RDD for the characteristic features of IgG4 sclerosis, including fibrosis, obliterative thrombophlebitis, lymphoplasmacytic infiltration, and specifically, the number of IgG4-positive plasma cells. Using immunohistochemistry (IHC) to identify these cells, we adopted a threshold of 30 IgG4-positive cells / HPF for an average of three HPF before ascribing IgG4 sclerosis.

Results: The seven patients' ages ranged from 11 to 70 years old. The ratio of females to males was 5:2. One patient had a history of autoimmune pancreatitis with elevated serum IgG4 levels; findings that have been linked to IgG4 sclerosis. Two patients had multiple lesion sites. Lymph node involvement was documented in two, but extranodal disease existed in all seven patients. Involved sites included the nasal cavity (2), the mediastinum (2), arm (2), skin (1), colon (1), and the subglottic region (1). Presenting symptoms varied from discrete masses and related sequelae to incidental discovery on radiographic imaging.

Six of the seven collected cases met or exceeded our established 30 IgG4 cells / HPF. IHC stains showed three-field-averages ranging from 30 – 146 IgG4-positive cells.

Conclusions: Our data showed a marked increase in IgG4 positive cells in six of seven RDD cases. This may suggest a possible close relationship between RDD and IgG4 sclerosing disease, but the relationship does not appear absolute. Further investigation and larger sample sizes are necessary to evaluate and define the relationship between RDD and IgG4 sclerosis.

85 Heparan Sulfate Is Required for Osteoblastic Lineage Commitment.

MI Wiweger, PCW Hogendoorn. Leiden University Medical Center, Netherlands.

Background: We have established a zebrafish (*Danio rerio*) model for multiple osteochondromas (MO), a syndrome caused by a mutation in the *EXT1* or *EXT2* genes leading to impaired biosynthesis of heparan sulfate. MO is mainly characterized by the development of benign cartilage-capped bone tumors at multiple sites of the skeleton. As shown in the zebrafish *dackel* (*dak*) mutant, heparan sulfate deficiency caused by a mutation in the *ext2* gene, affects cartilage organization and bone development. Interestingly, dermal bones (intra-membranous bones in mammals) that do not require a cartilage template are also malformed and often lost in the homozygote mutant. It is known that mammalian mesenchymal precursors can differentiate towards: i) chondrocytes, ii) osteoblasts, iii) muscles or iii) adipocytes. Previously, we have shown that differentiation of the chondrocytes is unaffected in the *dak* homozygote mutant. Here, we investigate if the impaired bone formation in the heparan sulfate-deficient fish might be explained by a switch in the commitment of osteoblast precursors towards fat and/or muscle cells.

Design: AB (wild type) and *dak* (*ext2*) homozygote mutant were raised under standard conditions. Fish were anesthetized in tricane, fixed in 4% formalin, dehydrated and stored in 100% methanol at -20 °C prior to use. Whole mount skeletons were stained with alizarin red and alcian blue. Fat deposition was visualized with Oil Red O. Expression patterns of osteoblast- and adipocyte-related markers were studied by whole mount mRNA *in situ* hybridization. Anti-MF20 antibody was used for muscle analysis. Light microscopy observations were performed on at least ten fish.

Results: Even though the muscles in heparan-deficient fish were shorter and more spaced out, as they fitted the misshapen cartilaginous skeleton, the overall musculature of the *dak* homozygote mutant was similar to that of WT. However, homozygote mutant fish showed a clear phenotype related to an abnormally high accumulation of lipids. No cartilage-, fat-, bone- nor muscle-related phenotypes were observed in the heterozygote *ext2* mutant. The molecular mechanisms underlying bone-to-fat switch are under investigation.

Conclusions: Heparan sulfate is involved in bone-to-fat switch during mesenchymal differentiation, without affecting chondrogenic- or muscle lineages. The presence of one functional copy of the *EXT2* gene is sufficient for the maintenance of normal osteoblast and adipocyte differentiation. Hence, MO patients are expected to manifest mosaic bone-to-fat switch at locations where either loss of heterozygosity or haploinsufficiency occurred.

86 KIT-Negative Gastrointestinal Stromal Tumor of the Abdominal Soft Tissue: A Clinicopathological and Genetic Study of 10 Cases.

H Yamamoto, Y Oda. Kyushu University, Fukuoka, Japan.

Background: Gastrointestinal stromal tumor (GIST) typically occurs in the digestive tract and express KIT protein associated with *KIT* or *platelet-derived growth factor receptor-alpha* (*PDGFRA*) gene mutation. Minor subset of GISTs are immunohistochemically negative for KIT, or occur in the soft tissue outside the gastrointestinal tract, namely extragastrointestinal stromal tumor (EGIST). Furthermore, KIT-negative EGISTs are very rare.

Design: We examined the clinicopathological and molecular characteristics of 10 cases of KIT-negative EGIST by using immunohistochemical stain and gene mutation analysis.

Results: The tumors occurred in omentum (n=5), mesentery (n=2), retroperitoneum (n=1), pelvic cavity (n=1) and not-otherwise-specified abdominal cavity (n=1). They ranged from 4 to 33 cm (median 15 cm) in maximum diameter with relatively low mitotic counts (median 3.5 per 50 high-power-fields). Morphologically, most cases were epithelioid cell (n=9) or mixed epithelioid and spindle cell (n=1) type, accompanied by variable amount of myxoid stroma. By immunohistochemical stain, the tumors were positive for CD34 (80%), PKC theta (90%) and DOG1 (90%), but negative for KIT

(0%). The majority of cases (7/9 cases tested; 78%) had *PDGFRA* mutations in exon 12 (n=1) or exon 18 (n=6). One case (11%) had the mutation in *KIT* exon 11, and the remaining one had no mutation in both *KIT* and *PDGFRA* genes.

Conclusions: The morphologic, phenotypic and genotypic features of KIT-negative EGIST are similar to those of KIT-negative gastric GIST. Although the origin of EGIST is debatable (really soft tissue primary vs. GI primary with secondary extension to soft tissue and eventual loss of connection to GI wall), KIT-negative EGIST should be considered as a potential abdominal soft tissue neoplasm. Immunohistochemical stain and molecular analysis are necessary not only to confirm the diagnosis but also to determine the therapeutic strategy.

87 Challenging Benign Fibro-Osseous Lesions of the Craniofacial Complex in Children.

M Yanes, J Mota, S Dickson, P Devilliers, H Rivera. Central University of Venezuela, Caracas, Venezuela; University of Alabama, Birmingham.

Background: Benign fibro-osseous lesions (BFL) are a group of developmental, reactive and neoplastic processes characterized by the replacement of normal bone by fibrous tissue. The WHO reclassified this group, in 2005, into ossifying fibroma, juvenile ossifying fibroma, fibrous dysplasia and osseous dysplasia. The purpose of this study was to analyze the histopathologic characteristics of BFL in children that may help avoid a misdiagnosis.

Design: A total of 4,500 cases from the 2000-2010 archives of the Oral Pathology Laboratory, Faculty of Dentistry, and 902 cases from the 1998-2010 archives of the Bone Pathology Section, Faculty of Medicine, Central University of Venezuela. All cases corresponding to BFL affecting children were selected. Data according to gender, anatomical location, histologic type and clinical diagnosis were analyzed. STATA (V.10.1) and SPSS (V.18) software and Fisher exact test were used for statistical analysis.

Results: There were ten cases of fibrous dysplasia (FD), six cases of ossifying fibroma (OF), and four of juvenile ossifying fibroma (JOF). The most common misdiagnosis was ossifying fibroma as fibrous dysplasia, due to lack of radiologic and clinical correlation. FD was most commonly observed among females during the first decade. OF was observed mostly in males while JOF was equally distributed. According to anatomic site, craniofacial FD was predominant, OF was most frequently observed in the mandible while JOF was present in the maxilla only.

Conclusions: The present study emphasizes the need to recognize these asymptomatic lesions during the first decade of life, which present with asymmetry, high recurrence rate and aggressive behavior. It is essential to correlate the radiologic, clinical and histologic features to avoid misdiagnosis.

88 Expression of Epithelial Markers in Nodular Fasciitis and Fibromatosis: An Immunohistochemical Study.

S Yasir, M Nadjji, P Kurzawa, GP Nielsen, A Rosenberg. University of Miami, Jackson Memorial Hospital, FL; Great Poland Cancer Centre, Poznan; Massachusetts General Hospital, Boston.

Background: Myofibroblasts are distinct cell type and share morphological and functional characteristics with fibroblasts and smooth muscle cells. Immunohistochemically, they express myogenic antigens and have been documented to stain with epithelial markers. Myofibroblasts participate in a variety of disease processes and are the dominant cell type in specific tumor-like proliferations and neoplasms including reactive lesions, such as nodular fasciitis (NF), benign indolent and locally aggressive neoplasms such as dermatofibroma and fibromatosis, respectively, and low and high-grade myofibroblastic sarcomas. In viscera, subtypes of carcinomas have been identified that mimic benign myofibroblastic lesions and because of the potential diagnostic pitfall that a keratin positive myofibroblastic tumor may introduce, we performed an immunohistochemical analysis to further explore the epithelial expression profile of well documented cases of nodular fasciitis and fibromatosis that arose in the soft tissues.

Design: Cases were identified from the surgical pathology files of Massachusetts General Hospital and consisted of resection specimens of 18 cases of nodular fasciitis and 20 cases of fibromatosis received between 2007 and 2010. A panel of 5 epithelial markers comprising CK-7, CAM5.2, AE1/AE3, P63 and estrogen receptor (ER) was performed on all cases. Cytoplasmic staining was assessed for the keratin antibodies and only nuclear immunoreactivity was considered positive for P63 and ER.

Results: Of eighteen cases of nodular fasciitis 9 were females (11-49 years) and 11 were males (5-69 years) with a mean age of 30.7 years (5-69 years). Of these eighteen cases 11 were located in upper extremity, 5 in head and neck, 1 in lower extremity and 1 in trunk. Of twenty cases of fibromatosis 14 were females (14-72 years) and 6 were males (15-28 years) with a mean age of 36.9 years (14-72 years). Of twenty cases 5 were located in lower extremity, 5 in trunk, 4 in shoulder, 3 in abdominal wall, 2 in buttocks and 1 in pelvis. All cases of nodular fasciitis (18/18) and fibromatosis (20/20) were negative for CK-7, CAM5.2, AE1/AE3, P63 and ER.

Conclusions: Nodular fasciitis and fibromatosis do not express epithelial immunohistochemical markers. Accordingly, a keratin positive tumor in which the differential diagnosis is between nodular fasciitis or fibromatosis and a variant of a spindle cell carcinoma is very unlikely to be one of these myofibroblastic proliferations.

89 MDM2 and CDK4 Are Coexpressed in a Subset of Extraskeletal Osteosarcoma.

A Yoshida, T Ushiku, T Motoi, M Fukuyama, H Tsuda, T Shibata. National Cancer Center, Tokyo, Japan; University of Tokyo, Japan; Teikyo University, Tokyo, Japan.

Background: *MDM2* and *CDK4* gene amplification and the resultant protein overexpression is a characteristic of the majority of well-differentiated/dedifferentiated

liposarcomas (WDLs/DDLS). Heterologous osteosarcomatous differentiation rarely occurs in WDLs/DDLS, and such a variant was previously shown to retain MDM2 and CDK4 immunohistochemical overexpression. Our recent encounter of a case of DDLS with massive osteosarcomatous differentiation, for which the diagnosis of extraskeletal osteosarcoma (ESOS) was seriously considered on initial biopsy, posed a question regarding the relationship between DDLS and ESOS. To clarify this, we undertook the immunohistochemical analysis of archival extraskeletal osteosarcomas.

Design: We retrieved 10 cases of extraskeletal osteosarcoma from the files of participating institutions (1960-2010). The tumor occurred in 7 men and 3 women, and the sites included retroperitoneum (n = 1), deep extremity (n = 4), superficial extremity (n = 3), pleura (n = 1), and ovary (n = 1). Nine cases were high-grade tumors; 1, low-grade. No cases showed histological/radiological evidence of coexistent liposarcomatous component. Visceral examples (n = 2) lacked coexisting carcinoma/mesothelioma or cytokeratin expression. A representative section of each case was immunostained with antibodies for MDM2 and CDK4. The results were expressed by staining intensity, which was graded from weak to strong, and by the extent of focal (1-10%) or diffuse (>10%) expression.

Results: Four (40%) cases were found to coexpress MDM2 and CDK4 mostly in a diffuse manner with moderate to strong intensity. They represented 50% of the 8 soft tissue ESOSs and 80% of the 5 deep-seated cases. One low-grade tumor was immunoreactive. The remaining 6 cases were negative for both the markers, and they included all the 3 superficially sited tumors and 2 visceral cases.

Conclusions: A subset of soft tissue ESOS, particularly when deep-seated, shows MDM2 and CDK4 coexpression. This subgroup may be related to DDLS despite the apparent lack of a coexisting liposarcomatous component.

90 MDM2 and CDK4 Coexpression and Coamplification Identifies among High-Grade Osteosarcomas a Distinct Subset Transformed from Low-Grade Osteosarcoma.

A Yoshida, T Ushiku, T Motoi, M Fukuyama, H Tsuda, T Shibata. National Cancer Center, Tokyo, Japan; University of Tokyo, Japan; Teikyo University, Tokyo, Japan.

Background: Low-grade osteosarcomas (LGOSs), namely, parosteal osteosarcoma and low-grade central osteosarcoma, are characterized by amplification of *MDM2* and *CDK4*, which results in overexpression of the encoded proteins. LGOSs may occasionally transform to higher grade sarcomas ("dedifferentiation"), which often take the form of high-grade osteosarcomas. Interestingly, previous studies have reported *MDM2* and *CDK4* amplification and/or overexpression in a minority (5-10%) of "conventional" high-grade osteosarcomas. We hypothesized that a high-grade osteosarcoma with *MDM2/CDK4* amplification and/or overexpression may actually represent a transformed osteosarcoma whose precursor low-grade component is unrecognized.

Design: Eighty-one consecutive untreated biopsy samples coded "high-grade osteosarcoma of the bone" were immunostained with antibodies for MDM2 and CDK4. Sixteen selected cases were also studied by quantitative real-time PCR for gene amplification status. Corresponding surgical resection materials of all the biopsy cases were subsequently reviewed to find out if low-grade osteosarcomatous component coexisted.

Results: Five (6%) cases showed coexpression of MDM2 and CDK4, and 2 of the 3 successfully studied cases harbored gene coamplification. Histological review of the resectates revealed low-grade component in 4 cases (80%), and the only tumor lacking the low-grade element showed focal weak immunoreactivity and no gene amplification. Of the remaining 76 cases, 5 (6%) were immunoreactive to either MDM2 or CDK4 alone, and 71 (88%) were negative for both MDM2 and CDK4. No gene amplification was detected in the 5 successfully studied cases lacking MDM2 and CDK4 coexpression; informative resection materials available for 57 cases revealed no coexisting low-grade component.

Conclusions: High-grade osteosarcomas rarely show MDM2 and CDK4 coexpression, and most positive cases, particularly when associated with gene amplification, correspond to those transformed from precursor low-grade osteosarcoma. Immunostaining may thus be useful in identifying a distinct subset of osteosarcoma, and contribute to the precise subclassification of this malignancy.

Breast

91 A New Pathological Response Index (PRI) for Neoadjuvant Chemotherapy Accurately Predicts Clinical Outcomes of Locally Advanced Primary Breast Cancers (LAPBC).

TMA Abdel-fatah, PM Mosley, A Lee, S Pinder, JS Reis-Filho, IO Ellis, SY Chan. School of Molecular Medical Science, Nottingham University City Hospitals, United Kingdom; Kings College London, Guy's and St Thomas' Hospitals, London, United Kingdom; Institute of Cancer Research, London, United Kingdom.

Background: Pathological complete response (pCR) after neoadjuvant therapy (NACT) predicts overall survival (OS). However, pCR is not a perfect surrogate for OS, given that a significant number of patients that do not achieve pCR benefit from chemotherapy. Furthermore, residual cancer cells after NACT includes a wide range of responses from near pCR to complete resistance.

Design: In this study we performed a comprehensive pathological assessment for 195 surgical specimens of LAPBC, removed after receiving anthracycline based chemotherapy with or without Taxane with long clinical follow-up (median > 10 years).

Results: A multivariate Cox regression model revealed that large size (>3cm) of the residual tumour (p=0.001), presence of lympho-vascular invasion (LVI) after NACT (p=0.004), absence of fibrotic reaction at the site of the primary tumour or lymph nodes